LIMNOLOGY and OCEANOGRAPHY

ASLO

Limnol. Oceanogr. 68, 2023, 982–1000

doi: 10.1002/lno.12325

Fluorescent properties of marine phytoplankton exudates and lability to marine heterotrophic prokaryotes degradation

Giancarlo Bachi,[1] Elisabetta Morelli,[1] Margherita Gonnelli,[1] Cecilia Balestra,[2] Raffaella Casotti,[3] Valtere Evangelista,[1] Daniel J. Repeta,[4] Chiara Santinelli [1,5*]

[1]Istituto di Biofisica, CNR, Pisa, Italy
[2]Istituto Nazionale di Oceanografia e Geofisica Sperimentale, Sgonico, TS, Italy
[3]Stazione Zoologica Anton Dohrn, Naples, Italy
[4]Department of Marine Chemistry and Geochemistry, Woods Hole Oceanographic Institution, Woods Hole, Massachusetts
[5]National Biodiversity Future Center (NBFC), Palermo, Italy

Abstract

Exudates by the diatom *Phaeodactylum tricornutum* were incubated with a natural community of marine heterotrophic prokaryotes for 24 d in order to investigate the link between the biological lability and the molecular weight, fluorescence, and polarity of phytoplankton dissolved organic matter (DOM). Dissolved organic carbon (DOC) removal, changes in fluorescence and in the heterotrophic prokaryote abundance were followed over time both in the total exudates and in the low- and high-molecular-weight fractions. To detect changes in the polarity of proteins, reverse-phase high-performance liquid chromatography (HPLC) was applied to the high-molecular-weight fraction. Our results indicate that freshly produced phytoplankton DOM exhibits a dynamic pattern of degradation that is accompanied by large changes in the growth efficiency of the bacterial community that are likely related to changes in DOM quality. Approximately 20% of high-molecular-weight DOM and 40% of fluorescence attributed to protein-like DOM were degraded over the first days of the incubation indicating that protein-like DOM is likely a labile component of phytoplankton exudates. In contrast, fluorescence measurements suggest that humic-like substances are resistant to bacterial degradation over the 24 d of the experiment. Despite fluctuations in the short-term rates of high-molecular-weight and low-molecular-weight DOM removal, the relative contributions of these fractions to DOM pool were similar in the fresh exudates and at the end of our incubation experiments.

Phytoplankton are the primary source of dissolved organic matter (DOM) to the oceans. During growth and after death, phytoplankton release a wide range of organic compounds, including carbohydrates (Myklestad 2000), amino acids, peptides and proteins (Granum et al. 2002), fatty and other organic acids (glycolate, tricarboxylic acids, and vitamins; Thornton 2014). It is well documented that phytoplankton are also one of the major sources of the chromophoric DOM (the fraction of DOM absorbing light; Stedmon and Markager 2005; Romera-Castillo et al. 2010; Kinsey et al. 2018) to the oceans. Phytoplankton phylogeny and adaptations to specific environmental conditions influence the chemical composition of the released DOM (Becker et al. 2014). Experiments with cyanobacteria (Bennette et al. 2011) and diatoms (Paul et al. 2009) have revealed that variability in phytoplankton exudates can be linked to growth stage (Barofsky et al. 2009; Vidoudez and Pohnert 2012), nutrient limitation (Bromke et al. 2013), and it is affected by the presence of co-cultured phytoplankton (Paul et al. 2009) or by the presence of specific bacterial populations (Grossart and Simon 2007).

Once released to the oceans, most phytoplankton DOM sustains heterotrophic metabolism and is respired to CO_2 or transformed into biomass. DOM that is rapidly respired or transformed into biomass is defined as labile (Hansell 2013). A minor fraction, defined as recalcitrant, escapes the rapid

*Correspondence: chiara.santinelli@ibf.cnr.it

Additional Supporting Information may be found in the online version of this article.

Author Contribution Statement: G.B.: conceptualizing, formal analysis, investigation, methodology, data curation, writing original draft. E.M.: investigation, formal analysis, methodology. M.G.: conceptualizing, investigation, methodology, data curation. C.B.: formal analysis. R.C.: formal analysis, data curation, resources. V.E.: formal analysis, data curation. D.J.R.: conceptualizing, investigation, resources. C.S.: accounted for the integrity of the data, analysis, and presentation of findings, conceptualization, investigation, resources, writing. All the authors contributed substantially to the final draft of the manuscript.

microbial removal and may accumulate for months to several millennia (Hansell 2013), playing a key role in carbon sequestration and export. Understanding the factors that determine the biological lability of phytoplankton DOM is therefore crucial for our understanding of the marine dissolved organic carbon (DOC) cycle.

In the last decades, many investigations have focused on the factors regulating the uptake of phytoplankton DOM by the heterotrophic prokaryotes (Grossart and Simon 2007; Romera-Castillo et al. 2010; Zheng et al. 2019). Lancelot (1984) observed that small metabolites can be used quickly, whereas complex polymers are not directly usable and although labile, have a longer residence time in seawater. Amon and Benner (1994) studied the bioavailability of high-molecular-weight DOM (HMWDOM) and low-molecular-weight DOM (LMWDOM) collected in the northern Gulf of Mexico during a diatom bloom and observed that bacterial growth and respiration were greater for the HMWDOM than for the LMWDOM. These authors formulated the size-reactivity continuum model suggesting that bulk HMWDOM is more bioreactive than bulk LMWDOM. Size per se does not appear to be the primary driver of the size-reactivity continuum. Indeed, the different size classes of organic matter have distinct chemical compositions influencing the rates of microbial degradation (Benner and Amon 2015). Even if today, it is known that distinct lineages of heterotrophic prokaryotes are adapted to metabolize specific pools of phytoplankton DOM (Grossart et al. 2005; Kieft et al. 2021), a holistic approach linking biological lability and molecular weight is still missing. Mechanistic model simulations agree with the size-reactivity continuum hypothesis (Mentges et al. 2019); studies linking molecular weight and biological lability are therefore crucial for the implementation of biogeochemical models aiming to constrain the reasons behind the persistence of DOM in the ocean (Zakem et al. 2021).

Another controversial point about phytoplankton DOM is the lability of its fluorescent fractions (fluorescent DOM [FDOM]). Only few studies followed the removal of phytoplankton FDOM (humic-like and protein-like substances) by heterotrophic prokaryotes with contrasting results. Laboratory incubations using *Synechococcus*-derived DOM, inoculated with a natural bacterial community, showed high lability of protein-like substances (Zheng et al. 2019), whereas other experiments suggest their substantial stability over 30 d of incubation (Romera-Castillo et al. 2011). Proteins are an important fraction of phytoplankton DOM (Myklestad 2000; Longnecker et al. 2015) and in the surface oceans they represent a highly bioavailable form of organic nitrogen (Sipler and Bronk 2015), supporting bacterial growth (20–65% of the bacterial N demand; Keil and Kirchman 1999). Proteins have characteristics fluorescence excitation and emission properties that have been used as proxy to study protein-like substances in the oceans (Jørgensen et al. 2011) and in laboratory experiments (Romera-Castillo et al. 2010, 2011; Zheng et al. 2019). To the best of our knowledge, there is no study linking the molecular characteristics of protein-like compounds, released by phytoplankton, to their biological lability. Two different scenarios can be hypothesized to explain their removal: (1) proteins are all degraded with the same rate, in this case microbial degradation equally consume them until a low subsistence concentration is reached and no difference is expected in their polarity or molecular weight during heterotrophic degradation; (2) there is a selective removal of proteins depending on their molecular characteristics, making some proteins escaping rapid bacterial uptake. In this case, polarity and molecular weight should change during heterotrophic degradation. Link fluorescence and lability is crucial since fluorescence is a fast, cheap and widely used technique capable to give information on DOM without sample pretreatment.

In the present study, exudates by the diatom *Phaeodactylum tricornutum* were incubated with a natural community of marine heterotrophic prokaryotes for 24 d, in order to investigate the link between the molecular weight, fluorescence and polarity of phytoplankton DOM, and uptake by heterotrophic prokaryotes. DOC removal, changes in fluorescence and in the heterotrophic prokaryote abundance were followed over time in the total exudates and in the low- and high-molecular-weight fractions. To detect changes in the polarity of proteins and link polarity with biological lability, reverse-phase high-performance liquid chromatography (HPLC) was applied to the high-molecular-weight fraction.

P. tricornutum, a pennate eukaryotic diatom, has received significant attention as a laboratory model organism (Butler et al. 2020). It has been used to study the chemical characteristic of phytoplankton DOM in comparison with other phytoplankton strains (Becker et al. 2014) as well as to study the fluorescent characteristics of hydrophobic DOM released by phytoplankton (Seritti et al. 1994). To the best of our knowledge, there is currently no information about the biological lability of DOM released by this strain.

Materials and methods

Phytoplankton cultures

The marine diatom *P. tricornutum* was obtained from the culture collection of algae and protozoa, Dunstaffnage Marine Laboratory. Stock cultures were grown in axenic conditions in a thermostatic chamber at 21 ± 1°C, under an illumination regime of 16 : 8 light : dark cycle, with fluorescent daylight at 100 μmol photons m^{-2} s^{-1}. The maintenance culture medium was natural seawater from an uncontaminated area of the Tyrrhenian Sea with f/2 enrichment, modified to f/10 for trace metal concentrations. Cells were maintained in exponential growth by inoculating them weekly into a fresh sterilized medium.

The culture medium used for the experiments characterizing exudate production was prepared with deep seawater (Eastern Mediterranean Sea; 2800 m; 34°45′07.3″N,

26°51′17.8″E), filtered through 0.2-μm membrane filters (Sartorius), enriched with f/2 medium. In order to have a low carbon medium and to avoid any DOC contamination (DOC concentration in the culture medium = 59 ± 2.4 μM), both vitamins and the trace metal were omitted from the f/2 recipe.

We carried out two experiments, the first in January 2019 (Exp1) and the second in June 2019 (Exp2; Fig. 1a). Algae from the stock culture were harvested by centrifugation (8000 × *g*, 10 min), washed two times with a fresh culture medium and inoculated at 1×10^5 cells mL^{-1} into 5-liter glass flasks (culture volume in each flask = 2 liters). We prepared 2 × 5-liter flasks for Exp1 and 4 × 5-liter flasks for Exp2 (Fig. 1a). The cultures were grown for 12 d under the same temperature and irradiance conditions as the stock cultures. In order to investigate the release of DOC and FDOM during growth, cell density, DOC, and fluorescence were measured in three flasks (one from Exp1 and two from Exp2) at $t = 0$ (inoculum) and after 2, 5, 8, and 12 d (total number of samples:

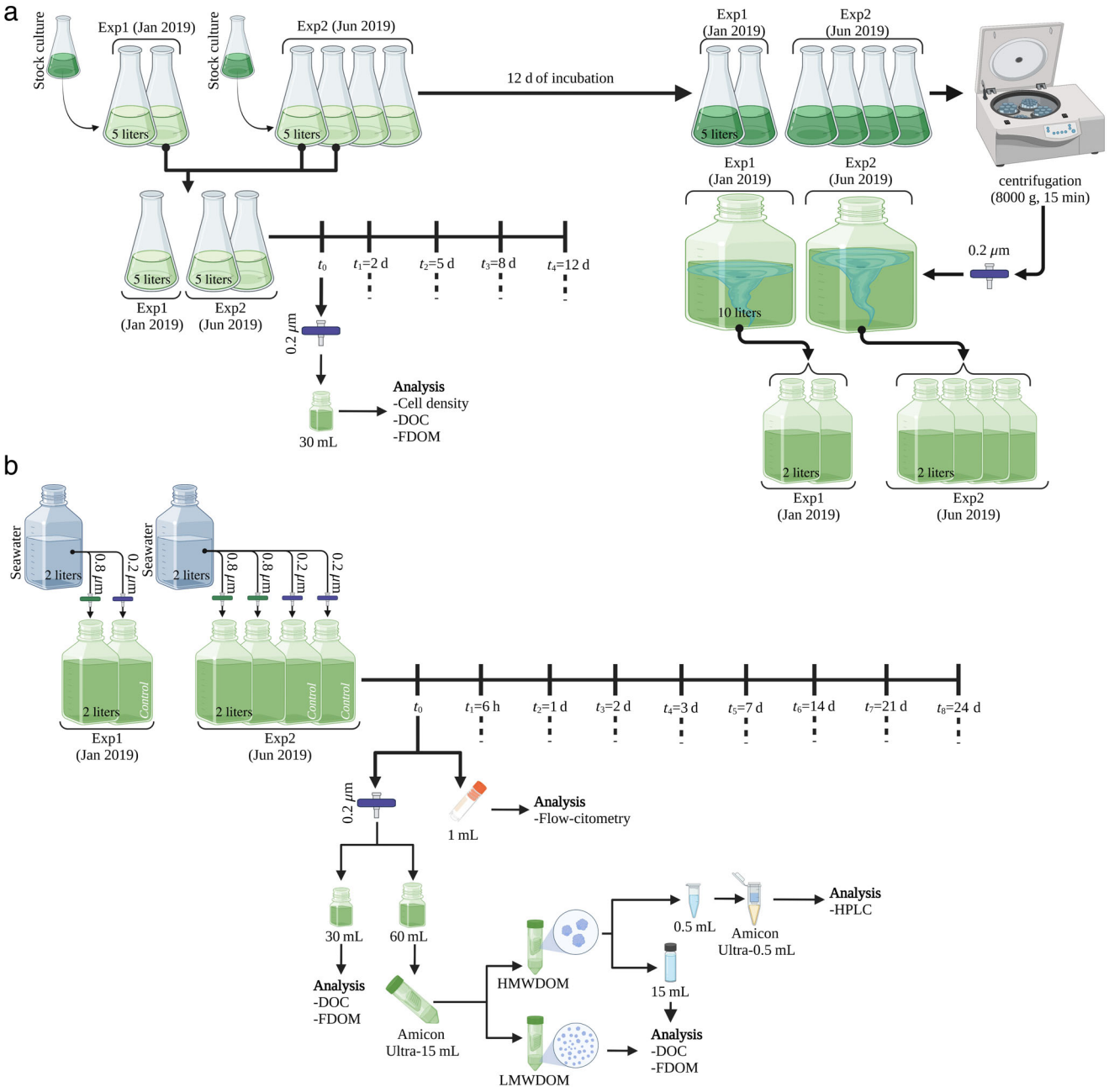

Fig. 1. Scheme of the culture (**a**) and incubation (**b**) experiments. The numbers on the bottles indicate their volume. Blue and green filters have a pore size of 0.2 and 0.8 μm, respectively. The sampling times are also indicated. Created with BioRender.com.

15). Finally, algae were removed by centrifugation (8000 × *g*, 15 min) and the supernatant was filtered through 0.2-μm nylon filters (WhatmanTM Polycap, 6705-3602 capsules; Fig. 1a). For each experiment, after the centrifugation, the supernatant from all the cultures was filtered into 1 × 10-liter acid-washed Nalgene bottle, gently mixed and then divided into 2-liter Nalgene bottles (two for Exp1 and four for Exp2) for the incubation experiments. This step allowed to homogenize the phytoplankton exudates before splitting it into replicates and controls bottles for the incubation experiment.

P. tricornutum cell density was measured by recording the absorbance of chlorophyll at 680 nm using a Jasco V-550 UV/vis spectrophotometer. A standard equation was established between optical density at 680 nm and cell numbers using a hemocytometer (Neubauer), under light microscopy (Zeiss).

Incubation experiment setup

For both Exp1 and Exp2, the exudates were collected in a 10-liter bottle, gently mixed and then divided into 2 × 2-liter bottles (Exp1) and 4 × 2-liter bottles (Exp2; Fig. 1b). All the bottles were polycarbonate (Nalgene) washed overnight with HCl (1%), rinsed with Milli-Q water overnight and autoclaved.

Water for the inoculum was collected at Marina di Pisa (Italy) filtered through a 0.8-μm filter (Sartorius Minisart®, 16592 K) into a 2-liter Nalgene bottle in order to exclude grazers and large cyanobacteria. It was gently mixed and then 0.2 liters were added into 1.8 liters of algal exudates (Fig. 1b). A control was designed to exclude any abiotic removal of DOM, 1.8 liters of the algal exudates were therefore inoculated with 0.2 liters of surface seawater collected at the same site, filtered through a 0.2-μm nylon filters (WhatmanTM Polycap, 6705-3602 capsules), and autoclaved, in order to remove all the microorganisms (Fig. 1b).

The bottles were incubated at 21 ± 1°C and in the dark for 24 d. Subsamples were collected immediately after the inoculation ($t = 0$), after 6 h, and then after 1, 2, 3, 7, 14, 21, and 24 d (total number of samples: 48). At each timepoint, 30 mL of subsample was filtered through a 0.2-μm filter and immediately analyzed for DOC and fluorescence (excitation–emission matrices [EEMs]), 60 mL of subsample was filtered through a 0.2-μm filter and immediately used for DOM fractionation. A subsample of 1 mL was collected for the measurement of heterotrophic prokaryote abundance (HPA; Fig. 1b). As reported above, two experiments were carried out, data from Exp1 (one replicate + one control) were merged with data from Exp2 (two replicates + two controls). The data from the three biological replicates for both the treatment and the control are presented as average ± standard deviation (Supporting Information Tables S3–S5). The good agreement among the three biological replicates, carried out at different times, allowed us to obtain robust results independent on the time they were carried out.

DOM fractionation by molecular weight

For DOM fractionation by molecular weight, a centrifugal filter device with a 3000 Da cut-off (Amicon Ultra-15 mL, Millipore) was centrifuged using an Eppendorf 5804R centrifuge (fixed angle rotor, 5000 × *g*, 30 min). The filtrate (molecular weight < 3000 Da, hereinafter LMWDOM) was collected and analyzed for both DOC and fluorescence (EEMs). One milliliter of the retentate (molecular weight > 3000 Da, hereinafter HMWDOM) was diluted with Milli-Q water to a volume of 15 mL and then analyzed for both DOC and fluorescence (EEMs; retention recovery > 95%). During Exp2, the remaining HMWDOM of the two replicates was mixed together and further concentrated with 3000 Da cut-off Amicon Ultra-0.5 mL (final volume ≅ 80 μL) and analyzed by HPLC. Before use, the Amicon Ultra-15-mL filters were washed with 0.1 N NaOH and rinsed with MilliQ water until the DOC and FDOM analyses confirmed the absence of any contamination. Samples for DOM fractionation were measured immediately after the collection.

DOC concentration

DOC concentration was measured by a Shimadzu TOC analyzer (TOC-Vcsn) by high-temperature catalytic oxidation. Samples were first acidified with HCl 2 N and sparged for 3 min with CO_2-free pure air in order to remove the inorganic CO_2. Samples (150 μL) were injected into the quartz combustion tube ($T \sim 680$°C) and the CO_2 produced was measured by a nondispersive infrared detector. From three to five injections were carried out until the analytical precision was lower than 2% (± 1 μM). A five-point calibration curve was carried out with standard solutions of potassium hydrogen phthalate in order to convert the signal of the CO_2 into μmol L^{-1} (μM). At the beginning and the end of each analytical day, the system blank was measured using Milli-Q water and the reliability of measurements was checked by comparison with a DOC consensus reference material (CRM; Hansell 2005; CRM Batch #18 nominal concentration of 42.5 ± 1.2 μM; measured concentration 43.2 ± 0.9 μM, $n = 52$).

Heterotrophic prokaryote abundance

One mL of subsample was collected from each bottle and fixed with glutaraldehyde (0.05% final concentration) and stored at −80°C for HPA measurements. HPA was determined by flow cytometry (Balestra et al. 2011). Thawed samples were stained with SYBR Green I (Molecular Probes) for 10 min in the dark at room temperature and analyzed using a FACSVerse flow cytometer (BD BioSciences), equipped with standard filters and laser. HPA was counted on the side scatter vs. FL1 (green fluorescence) plots after gating.

HPA was transformed into HP Biomass Carbon (HPB-C) by multiplying cell numbers by 20 fg C $cell^{-1}$ (Fukuda et al. 1998). Heterotrophic prokaryote growth efficiency (HPGE) was estimated as follows:

$$\mathrm{HPGE} = \frac{\Delta\mathrm{HPB} - \mathrm{C}}{\Delta\mathrm{DOC}} \times 100$$

where ΔHPB-C is the change in HPB-C and ΔDOC is the change in DOC concentration, calculated during the exponential growth phase.

FDOM fluorescence and parallel factor analysis

EEMs were obtained by using the Aqualog spectrofluorometer (HORIBA Jobin Yvon) with a 10 × 10-mm quartz cuvette. This instrument uses a charge-coupled device to detect the signal, guaranteeing a high acquisition velocity and reduced photobleaching. The characteristics of the lamp improve the sensibility of data acquisition at low excitation wavelengths (250–350 nm) allowing a better identification of the protein-like fluorescence. Emission was registered between 212 and 620 nm every 3.27 nm (8 pixels) with an integration time of 10 s, but only the data between 250 and 620 nm were taken into consideration. Excitation ranged between 250 and 450 nm at 5 nm increment. EEMs were corrected for instrumental bias and subtracted from the EEM of the sterilized (by filtration) culture medium. Rayleigh and Raman scatter peaks were removed by using monotone cubic interpolation. The EEMs were elaborated using the TreatEEM software (Omanovic Dario, TreatEEM-program for treatment of fluorescence EEMs, http://sites.google.com/site/daromasoft/home/treateem).

EEMs were corrected for the inner filter effect using the following equation:

$$F_{\mathrm{corr}} = F_{\mathrm{obs}} 10^{\frac{\mathrm{Abs_{Ex}} + \mathrm{Abs_{Em}}}{2}}$$

where F_{corr} is the inner filter effect corrected fluorescence intensity, F_{obs} is the measured fluorescence intensity, $\mathrm{Abs_{Ex}}$ is the absorbance at fluorescence excitation wavelength, and $\mathrm{Abs_{Em}}$ is the absorbance at the selected fluorescence emission wavelength. Absorbance was measured by the Aqualog spectrofluorometer (HORIBA Jobin Yvon) on the same sample used for fluorescence analysis. The corrected EEMs were normalized dividing the fluorescence intensity by the Raman band of Milli-Q water integrated between 371 and 428 nm (λ_{Ex} = 350 nm). Fluorescence was therefore reported in Raman Units (Lawaetz and Stedmon 2009).

Parallel factor (PARAFAC) analysis was applied to the 107 EEMs using the decomposition routines for EEMs toolbox for MATLAB software (Murphy et al. 2013). PARAFAC validated a five-component model, meaning that five main groups of fluorophores characterize the FDOM pool. The OpenFluor online database, a database of environmental fluorescence spectra, was used as a validation tool to characterize the five components. OpenFluor compares excitation and emission spectra of the validated components with all the components present in the database and allows to compare the spectra by using the Tucker congruence coefficient (TCC; Murphy et al. 2014).

Component 1 ($\lambda_{\mathrm{Ex}}/\lambda_{\mathrm{Em}}$: 280 [370, 430]/528 nm) showed spectroscopic characteristics similar to the riboflavin (vitamin B2) and its derivate lumichrome (Yang et al. 2016). A search of the OpenFluor database did not find any match with Component 1's excitation and emission spectrum. Here, we characterize Component 1 as Flavin-like (**$\mathbf{C1_{Flv\text{-}like}}$**) based on its excitation/emission characteristics. **Component 2** ($\lambda_{\mathrm{Ex}}/\lambda_{\mathrm{Em}}$: 280/331 nm) showed spectroscopic characteristics similar to Coble's peak *T* ($\lambda_{\mathrm{Ex}}/\lambda_{\mathrm{Em}}$: 275/340 nm; Coble 1996). The OpenFluor database found 25 matches (TCC > 0.95) with its excitation and emission spectrum. Component 2 was characterized as Tryptophane-like (**$\mathbf{C2_{Trp\text{-}like}}$**). **Component 3** ($\lambda_{\mathrm{Ex}}/\lambda_{\mathrm{Em}}$: 255 [355]/442 nm) showed spectroscopic characteristics similar to Coble's peaks C and A ($\lambda_{\mathrm{Ex}}/\lambda_{\mathrm{Em}}$: 350/451 and 245/451 nm, respectively; Coble 1996). OpenFluor online database found 28 matches (TCC > 0.95) with its excitation and emission spectrum. Component 3 was characterized as humic-like (**$\mathbf{C3_{H1\text{-}like}}$**). **Component 4** ($\lambda_{\mathrm{Ex}}/\lambda_{\mathrm{Em}}$: 295/396 nm) showed spectroscopic characteristics similar to Coble's peak M ($\lambda_{\mathrm{Ex}}/\lambda_{\mathrm{Em}}$: 312 [380]/420; Coble 1996; Coble et al. 1998). The OpenFluor online database found 14 matches (TCC > 0.95) with its excitation and emission spectrum. Component 4 was characterized as humic-like (**$\mathbf{C4_{H2\text{-}like}}$**). **Component 5** ($\lambda_{\mathrm{Ex}}/\lambda_{\mathrm{Em}}$: 260/305 nm) showed spectroscopic characteristics similar to Coble's peak B ($\lambda_{\mathrm{Ex}}/\lambda_{\mathrm{Em}}$: 275/310 nm; Coble 1996). OpenFluor database found three matches (TCC > 0.95) with its excitation and emission spectrum. Component 5 was characterized as Tyrosine-like (**$\mathbf{C5_{Tyr\text{-}like}}$**). For further details on the characteristics of the components, see the Supporting Information (Fig. S1; Table S1).

Reverse-phase HPLC fractionation of HMWDOM

Analyses of the samples collected during Exp2 were performed by HPLC consisting of two Shimadzu LC-10 AD pumps, a Rheodyne 7725 injection valve equipped with a 50 μL loop, a fluorescence detector (RF–10AXL, Shimadzu) set at 280 nm excitation wavelength and 350 nm emission wavelength, and a Kinetex (Phenomenex) 2.6 μm C18 reverse phase column (100 mm × 4.6 mm). A stepwise gradient using 0.1% aqueous trifluoroacetic acid as solvent A and 100% acetonitrile as Solvent B was used at a flow rate of 1 mL min^{-1}. The proportion of solvent B increased from 0% to 100% following the gradient shown in Supporting Information Fig. S2 and Table S2.

Exponential fitting with a constant curve

DOC removal over time was fitted into an exponential with a constant curve using the following equation:

$$y = A_1^{(-x_{t1})} + Y_0$$

where Y_0 is the offset, A_1 is the amplitude, and t_1 is the time constant. The exponential model was carried out using the

software OriginPro, Version 9 (OriginLab Corporation). The half-life time ($t_{1/2}$) was calculated as $\ln_{(2)}t_1$.

Statistical analysis

Differences in the treatments for all the parameters were tested using the Kruskall–Wallis nonparametric test. Differences were considered significant at the threshold of $p < 0.05$. All statistical analysis were performed using OriginPro, Version 9 (OriginLab Corporation).

Results

Release of DOC and FDOM by *P. tricornutum*

P. tricornutum cell density increased exponentially from $1.0 \pm 0.1 \times 10^5$ cells mL^{-1} at day 0 to $1.8 \pm 0.1 \times 10^6$ cells mL^{-1} at day 5, when it reached the stationary phase (Fig. 2a). DOC concentrations increased steadily throughout the exponential and stationary phase from 59 ± 1.6 μM at day 0 to 225 ± 0.5 μM at day 12 (Fig. 2b).

The EEMs of the exudates at day 0 showed only a small $C2_{Trp\text{-}like}$ peak (Fig. 3a), whereas after 12 d a marked increase in both $C2_{Trp\text{-}like}$ and $C3_{H1\text{-}like}$ peaks was observed (Fig. 3d), together with the appearance of a $C1_{Flv\text{-}like}$ peak (Fig. 3d). $C2_{Trp\text{-}like}$ increased in the first 2 d (Fig. 2d), before the appearance of $C3_{H1\text{-}like}$ and $C1_{Flv\text{-}like}$ peaks between days 2 and 5 (Fig. 3c). The highest increase in fluorescence was observed between days 2 and 5 for $C2_{Trp\text{-}like}$ (Fig. 2d), between days 2 and 8 for $C3_{H1\text{-}like}$ (Fig. 2e) and between days 2 and 12 for $C1_{Flv\text{-}like}$ (Fig. 2c).

EEMs of the phytoplankton DOM fractionated by molecular weight

At day 12, the DOC concentration was 225 ± 0.5 μM in the total exudate, 168 ± 0.8 μM in the LMWDOM, and 56 ± 0.4 μM

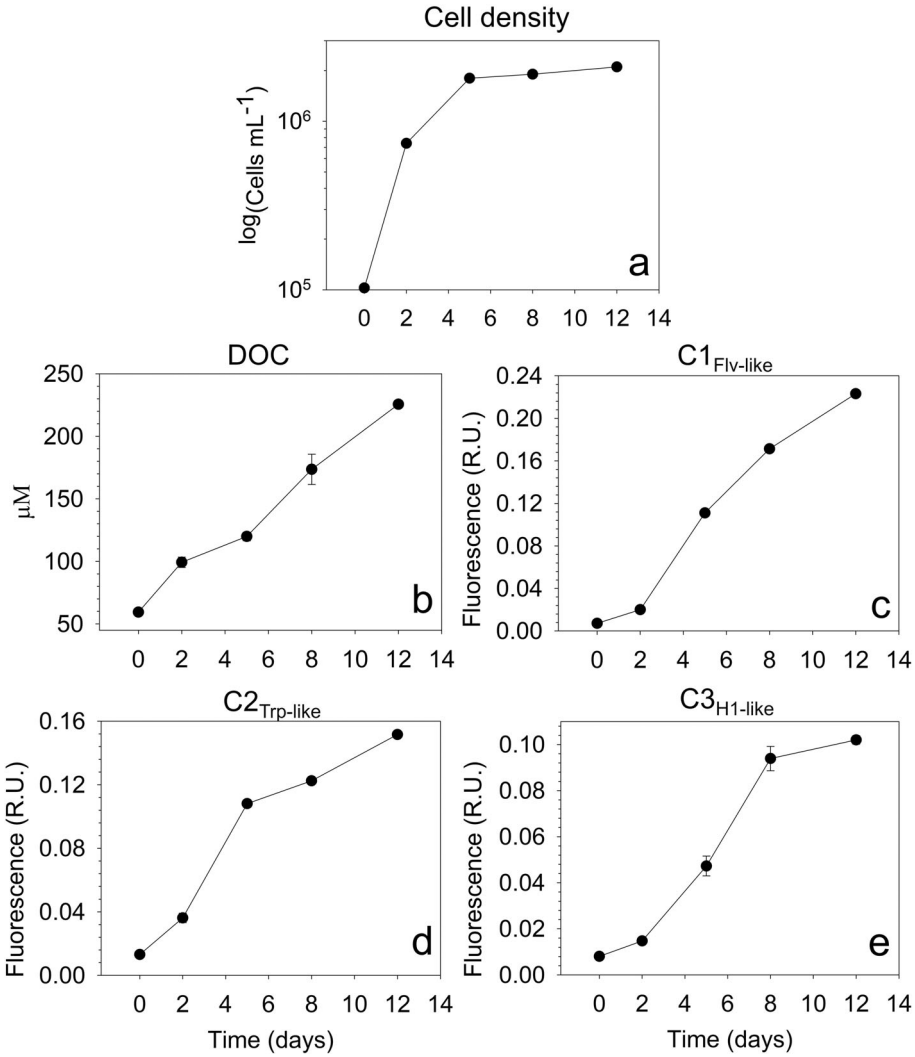

Fig. 2. *Phaeodactylum tricornutum* cell density (**a**), DOC concentration (**b**) and fluorescence intensity of $C1_{Flv\text{-}like}$ (**c**), $C2_{Trp\text{-}like}$ (**d**), and $C3_{H1\text{-}like}$ (**e**) during exponential and stationary growth phases (0–12 d). $C2_{Trp\text{-}like}$ and $C3_{H1\text{-}like}$ were taken as representative of protein-like and humic-like components, respectively. The error bars refer to the standard deviation among the three biological replicates. The error bars are reported for each point, note that sometimes they are not visible because the standard deviation is too small.

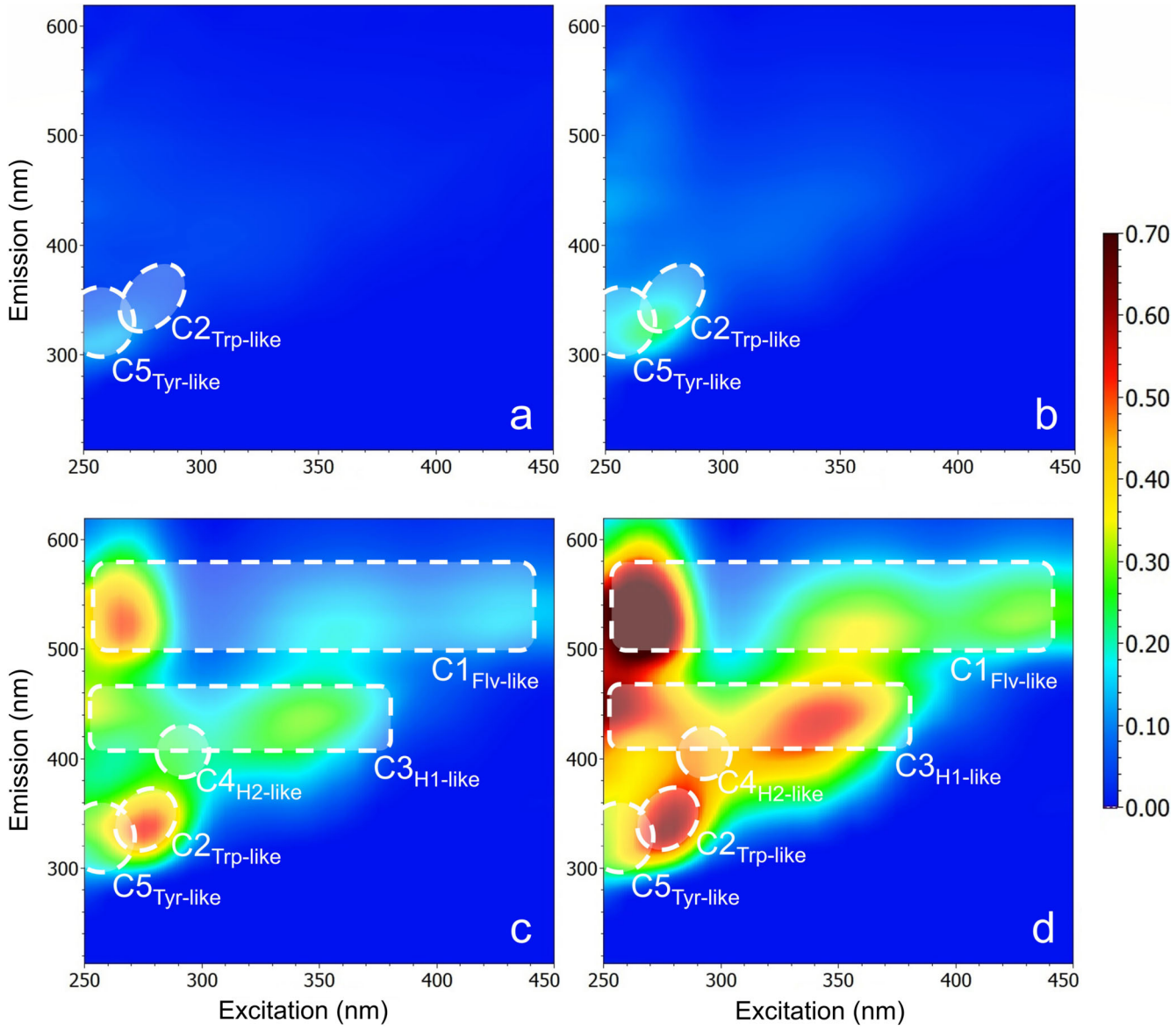

Fig. 3. EEMs of the exudates of *Phaeodactylum tricornutum* at days 0 (**a**), 2 (**b**), 5 (**c**), and 12 (**d**). The colors refer to the fluorescence intensity expressed in Raman Units (R.U.). The dashed boxes indicate the location of the components. EEMs are the average of the EEMs of the three biological replicates of the culture.

in the HMWDOM, indicating that 75% of phytoplankton DOC was low molecular weight (< 3000 Da), and only 25% was high molecular weight (> 3000 Da).

EEMs of the total exudates (Fig. 4a), LMWDOM (Fig. 4b), and HMWDOM (Fig. 4c) showed a separation of fluorophores, with most of $C1_{Flv\text{-}like}$, and humic-like components ($C3_{H1\text{-}like}$ and $C4_{H2\text{-}like}$) as well as a small amount of protein-like ($C2_{Trp\text{-}like}$ and $C5_{Tyr\text{-}like}$) appearing in the LMWDOM fraction (Fig. 4b) and most of protein-like components ($C2_{Trp\text{-}like}$ and $C5_{Tyr\text{-}like}$) retained in the HMWDOM fraction (Fig. 4c).

HPA and DOC trend during the incubation experiments

After an initial 24-h lag phase, heterotrophic prokaryotes grew exponentially until day 20, with cell numbers increasing from $7.0 \pm 1.7 \times 10^4$ to $7.4 \pm 0.5 \times 10^6$ cells mL^{-1} (Fig. 5), then the stationary phase was reached and HPA remained stable until the end of the incubation (day 24). At the beginning of the incubation, the addition of 10% costal seawater (inoculum; DOC = 85 μM), decreased the DOC concentration by 9 μM (from 225 to 216 μM), highlighting that no contamination occurred during the manipulation of the samples. Immediately after inoculation (day 1), a 15 μM DOC decrease was observed. Between days 2 and 20, DOC decreased from 201 ± 0.3 to 151 ± 7.5 μM, in correspondence with an increase in HPA. No significant change was observed between days 20 and 24 (Fig. 5). Taking into consideration, the 24 d of incubation, 30% of the initial DOC pool was removed. In the control, a slight increase in HPA was observed at day 24, but

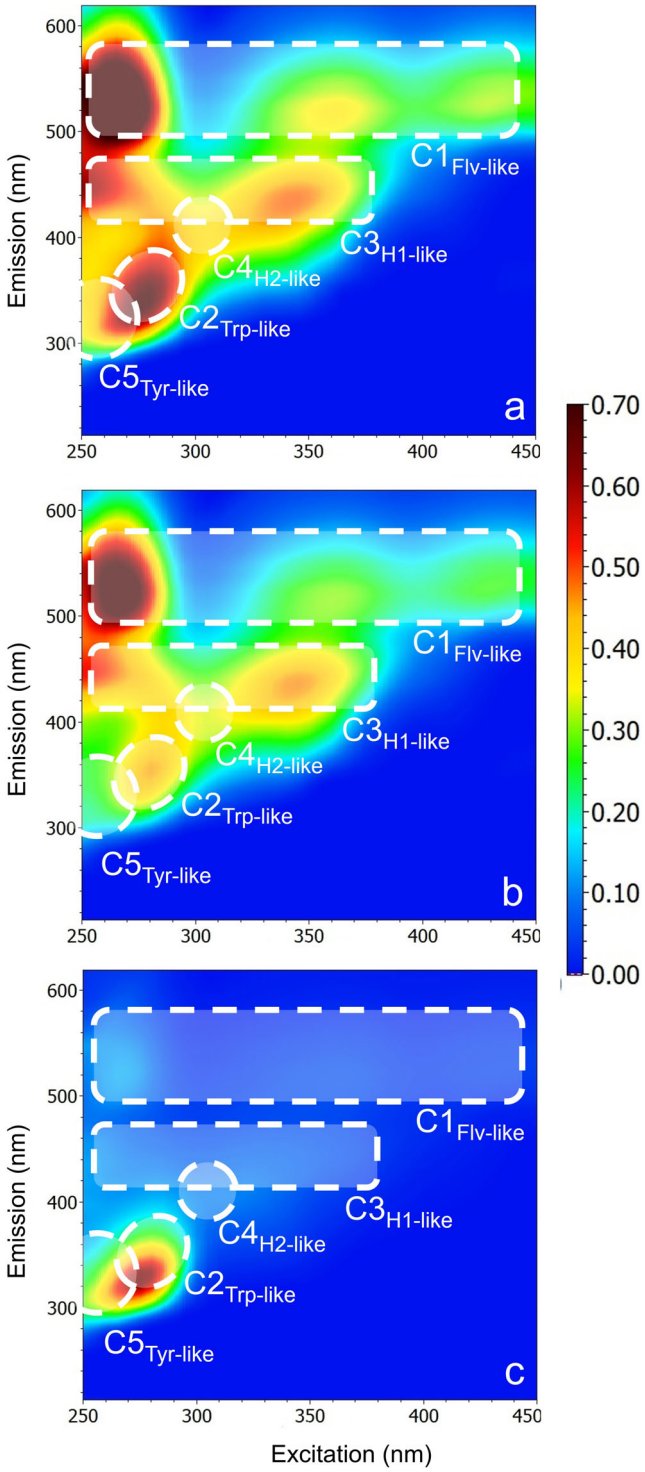

Fig. 4. EEMs of the (**a**) total exudate, (**b**) LMWDOM, and (**c**) HMWDOM before the inoculation with a natural assemblage of marine heterotrophic prokaryotes. The colors refer to the fluorescence intensity expressed in Raman Units (R.U.). The dashed boxes indicate the location of the components. EEMs are the average of the EEMs of the three biological replicates of the culture.

the value was fourfold lower than in the treatment and no significant difference was observed for DOC concentration,

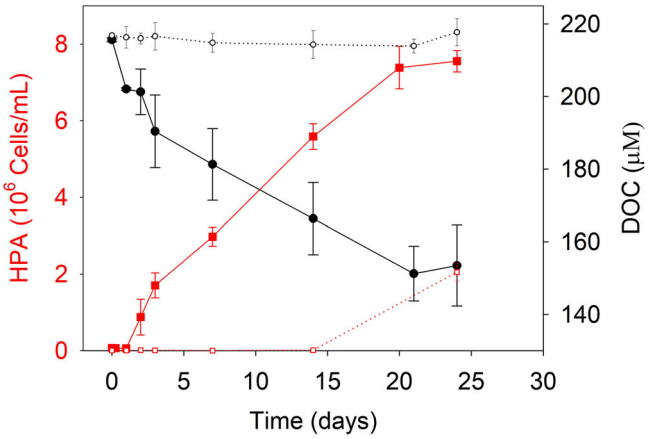

Fig. 5. DOC (black line and circles) and HPA (red line and squares) during the 24-d incubation. The dotted lines represent the control for DOC (black circles) and HPA (red squares). The error bars refer to the standard deviation among the three biological replicates both in the treatment and in the control.

indicating that this increase in HPA only minimally impacted DOC utilization. DOC removal rates changed during the incubation: between days 0 and 3 the removal rate was 8.3 μM d^{-1}, between days 3 and 24 the removal rate decreased to 1.8 μM d^{-1}. In the total exudate, ~ 25 μM (11%) were removed during the first 3 d and 37 μM (17%) between days 3 and 14 (Figs. 5, 6a). In the LMWDOM fraction incubation, 14 μM (7%) was removed in the first period (4.6 μM d^{-1}) and 37 μM (20%) in the second period (1.8 μM d^{-1}; Fig. 6b). In the HMWDOM fraction incubation, 11 μM (19%) was removed in the first period (3.7 μM d^{-1}), whereas in the second period no decrease was observed in DOC concentration (Fig. 6c).

DOC concentrations over time in the total exudate, LMWDOM and HMWDOM factions were fitted to an exponential curve (Fig. 6; Table 1). The exponential fitting indicates that the average DOC removed in 24 d (A_1), that is, the fraction labile on this temporal scale, had similar values for the total exudate and the LMWDOM (65 ± 6 and 66 ± 11 μM, respectively) and it was much lower for the HMWDOM (11 ± 2 μM). The offset (Y_0), that is, the DOC that was not removed in 24 d was 146 ± 7 μM in the total exudate, 93 ± 12 μM in the LMWDOM, and 45 ± 1 μM in the HMWDOM. The half-life time ($t_{1/2}$), that is the estimated time needed to remove 50% of the fraction lost during the incubation, considered as labile DOC (i.e., the difference between the initial concentration and Y_0), was 7.2 d for the total exudate, 10.7 d for LMWDOM, and only 0.5 d for HMWDOM (Table 1).

FDOM in the total exudate

In the total exudate, $C1_{Flv\text{-}like}$ did not show significant changes during the first 3 d of incubation and then decreased between days 3 and 20 (Fig. 7a), a decrease in the control was also observed between days 7 and 14. After 2 d without

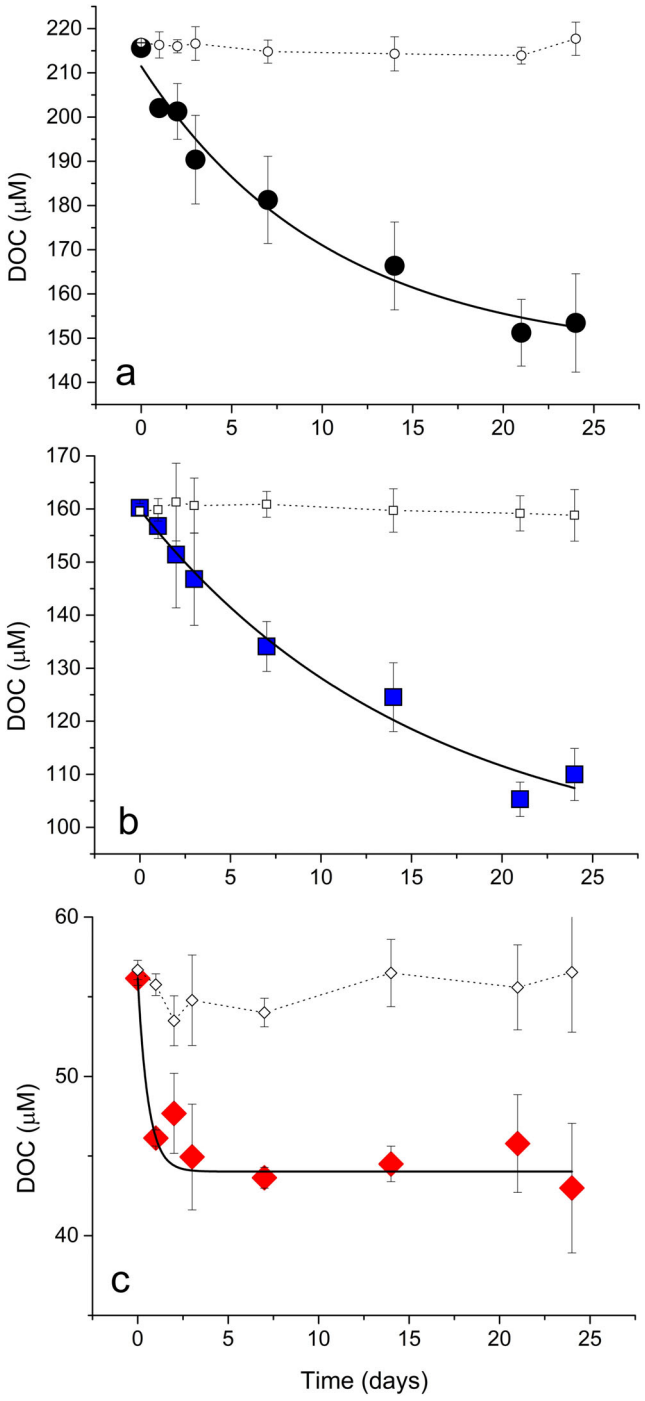

Fig. 6. Fitting of the observed DOC trend with an exponential model (Table 1) in the (**a**) total DOM, (**b**) LMWDOM, and (**c**) HMWDOM of the treatments (black dots, blue square, and red diamonds) and their respective controls (empty dots, squares, and diamonds).The error bars refer to the standard deviation among the three biological replicates.

significant changes, $C2_{Trp\text{-}like}$ rapidly decreased (−40%) until day 14 and then continued to slowly decrease during the last 10 d of the experiment (Fig. 7c).

Table 1. Exponential fitting of the DOC trend in the total DOC, LMWDOM, and HMWDOM. Y_0 (μM) indicates the concentration of the DOC that was not removed in 24 d (recalcitrant DOC), A_1 (μM) indicates the total amount of DOC removed during the incubation (labile DOC), and $t_{1/2}$ (days) refers to the half-life time of the DOC removed during the incubation.

$y = A_1^{(-x/t1)} + y_0$

	Y_0 (μM)	A_1 (μM)	$t_{1/2}$ (d)	R^2
Total DOC	146 ± 7	65 ± 6	7.2 ± 2.1	0.97
LMWDOM	93 ± 12	66 ± 11	10.7 ± 4	0.97
HMWDOM	45 ± 1	11 ± 2	0.5 ± 0.2	0.86

$C3_{H1\text{-}like}$ increased slightly during the first 3 d of incubation and then remained nearly constant until day 24 (Fig. 7e). $C4_{H2\text{-}like}$ increased during the first 7 d of incubation, then decreased between days 7 and 14, when it went back to its initial value. During the last 10 d of incubation, $C4_{H2\text{-}like}$ did not show any significant change (Fig. 8a). $C5_{Tyr\text{-}like}$ rapidly increased during the first 3 d of incubation, decreased between days 3 and 14, after which it did not show significant changes until the end of incubation (Fig. 8c), when values were similar to the initial ones. In the control, no variation was observed for $C2_{Trp\text{-}like}$, $C3_{H1\text{-}like}$, $C4_{H2\text{-}like}$, and $C5_{Tyr\text{-}like}$ (Figs. 7b,d,f, 8b,d).

Fluorescence of the low-molecular-weight fraction

In the low-molecular-weight fraction, $C1_{Flv\text{-}like}$ decreased between days 1 and 14, following a trend similar to that observed in the total exudates (Fig. 7a). A similar decrease was also observed in the control but only until day 7 (Fig. 7b), suggesting that in the first part of the incubation abiotic processes are the main players in the removal of this fraction. The $C2_{Trp\text{-}like}$ increased during the first 7 d of the incubation and then decreased until the end of incubation (Fig. 7c). $C3_{H1\text{-}like}$ increased slightly during the incubation, reaching the highest values at day 21 as observed in the total exudates (Fig. 7e). $C4_{H2\text{-}like}$ increased during the first days of the incubation and then decreased between days 7 and 14 (Fig. 8a), following the trend observed in the total exudates. $C5_{Tyr\text{-}like}$ increased during the first days of incubation as seen for the total exudate and then remained stable for the rest of the incubation (Fig. 8c). In the control, no variation was observed for $C2_{Trp\text{-}like}$, $C3_{H1\text{-}like}$, $C4_{H2\text{-}like}$, and $C5_{Tyr\text{-}like}$ (Figs. 7b,d,f, 8b,d).

Fluorescence of the high-molecular-weight fraction

$C1_{Flv\text{-}like}$, $C3_{H1\text{-}like}$, and $C4_{H2\text{-}like}$ were almost absent (near the detection limit of the instrument) in the high-molecular-weight fraction, indicating that most of the humic-like material was in the low-molecular-weight fraction (Fig. 7a,e, 8a). $C2_{Trp\text{-}like}$ markedly decreased after the inoculation showing high lability of protein-like molecules larger than 3000 Da

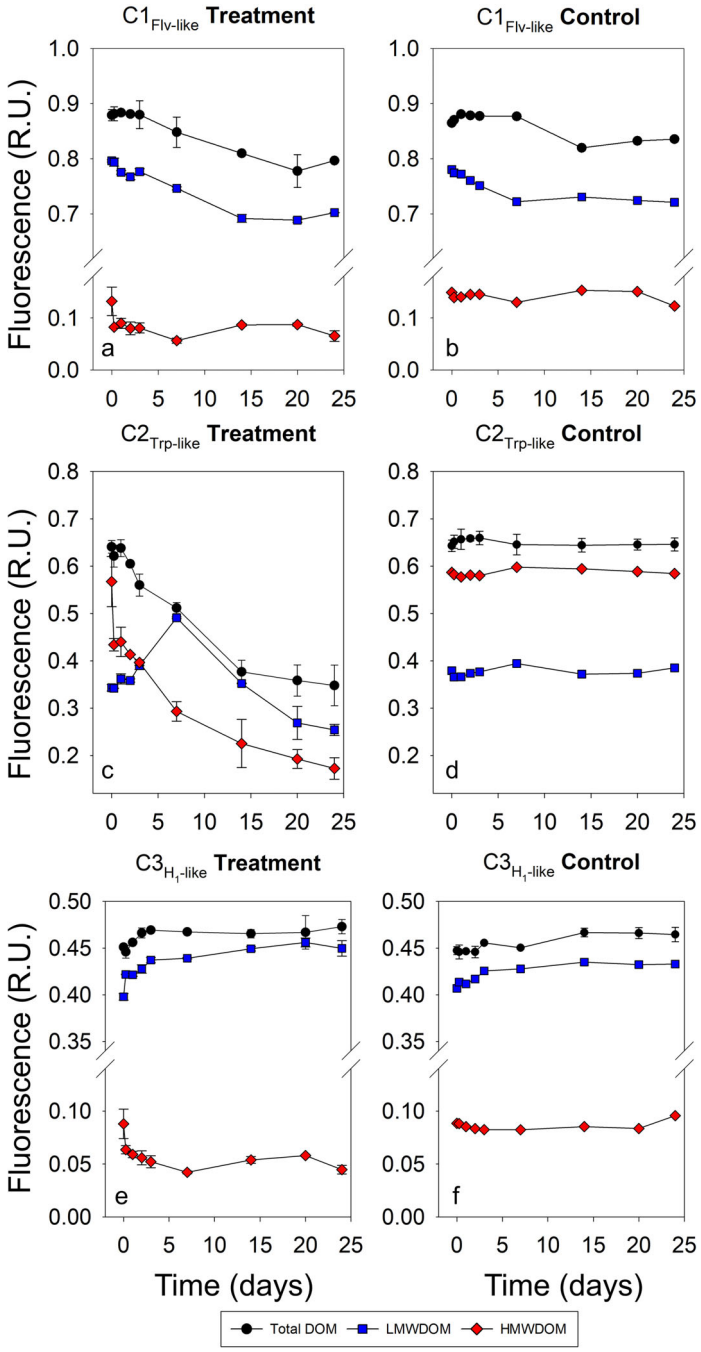

Fig. 7. Fluorescence intensity of the components $C1_{Flv\text{-}like}$, $C2_{Trp\text{-}like}$, and $C3_{H1\text{-}like}$ identified by PARAFAC analysis during the 24 d incubations with heterotrophic prokaryotes in the total DOM (black), LMWDOM (blue), and HMWDOM (red, left panels) compared with the control (right panels). The error bars in the treatment refer to the standard deviation among the three biological replicates.

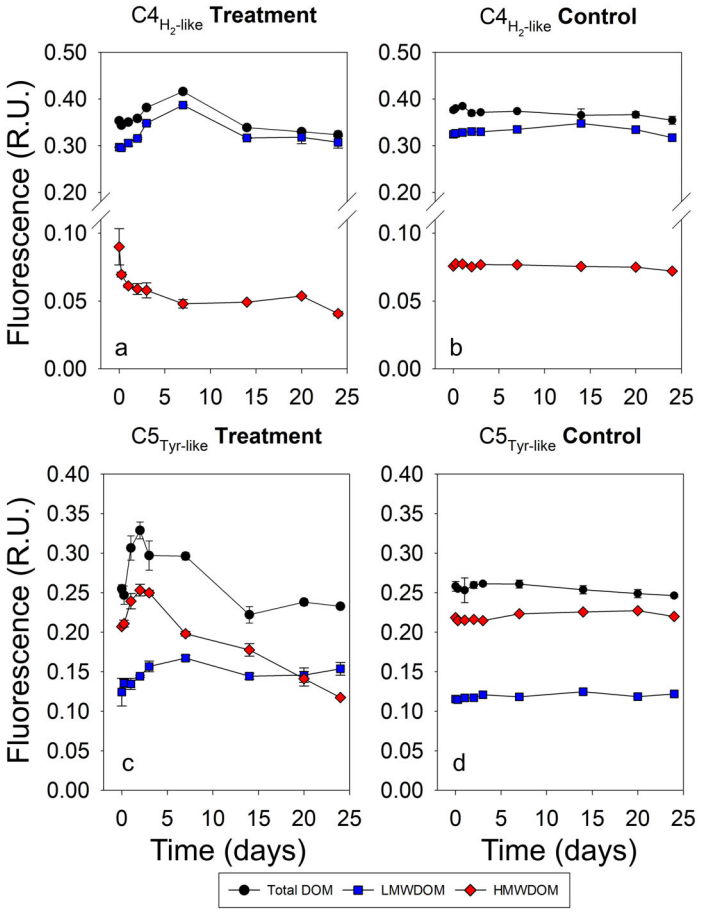

Fig. 8. Fluorescence intensity of the components $C4_{H2\text{-}like}$ and $C5_{Tyr\text{-}like}$ identified by PARAFAC analysis during the 24 d incubations with heterotrophic prokaryotes in the total DOM (black), LMWDOM (blue), and HMWDOM (red, left panels) compared with the control (right panels). The error bars in the treatment refer to the standard deviation among the three biological replicates.

(Fig. 7c). $C5_{Tyr\text{-}like}$ increased between days 0 and 3 and then decreased until the end of the incubation (Fig. 8c). It is noteworthy that at the end of the incubation the fluorescence intensity of both $C2_{Trp\text{-}like}$ and $C5_{Tyr\text{-}like}$ was lower in the HMWDOM than in the LMWDOM, despite it was higher at the beginning of the incubation.

Characterization of fluorescent compounds in HMWDOM by HPLC

Typical chromatograms of concentrated HMWDOM are shown in Fig. 9 both for the heterotrophic prokaryotes enriched samples (treatment) and for the control. Each increase in solvent B (acetonitrile) along the step gradient washed a protein-containing fraction off the column. The five separated protein fractions responded differently in the incubation experiment. The relative abundance of the nonpolar fractions at 5.2, 4.2, and 3.8 min decreased immediately after inoculation and continued to decrease during the rest of the incubation. The peak at 2.9 min markedly decreased after 6 h of incubation and remained low for the rest of the incubation. The peak at 2.5 did not change for the first 3 d of incubation and then increased at day 7 in correspondence with the

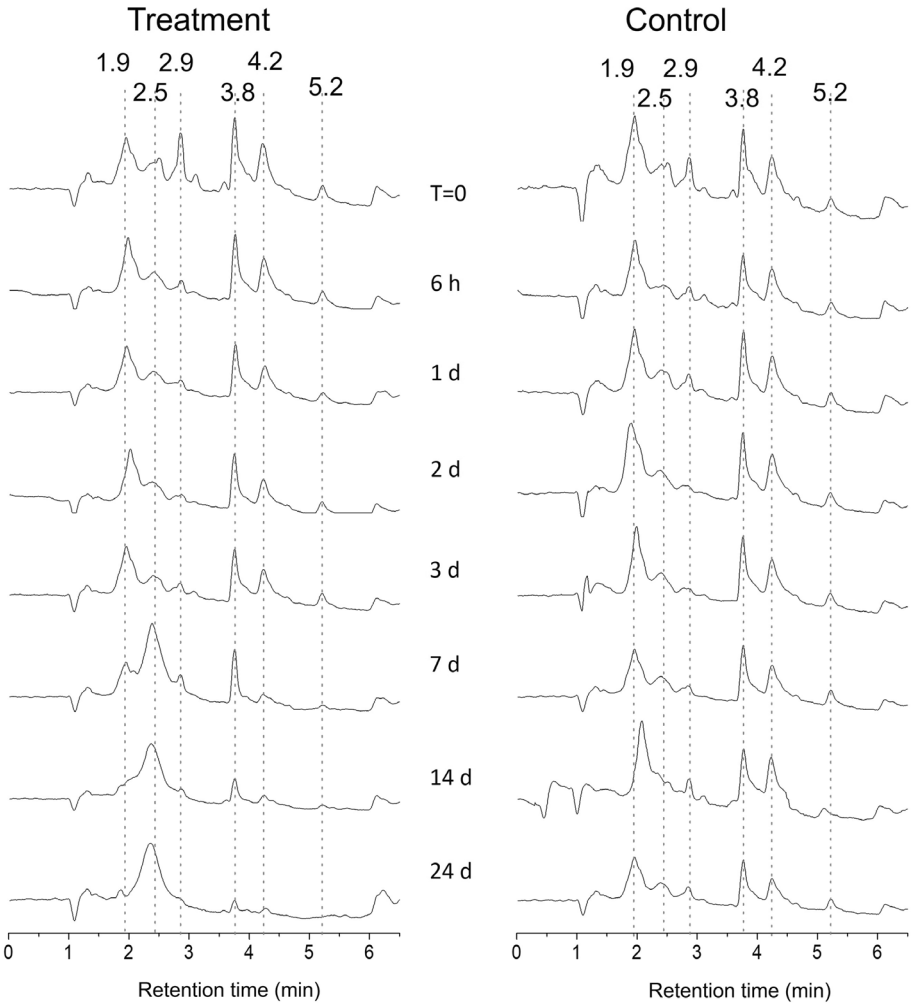

Fig. 9. Chromatograms of the HMWDOM in the treatment (left panels) and in the control (right panels) at the different incubation times. The dotted lines indicate the peaks of the fractions separated by polarity and are reported as a visual aid to align peaks among the chromatograms.

decrease of the most polar peak at 1.9 min. In contrast, peaks in the chromatograms of the control samples exhibited only minor modifications in the intensity of the peaks over time but not in the position of the peaks, indicating that, in the control the hydrophobicity of the high-molecular-weight exudates did not change over time (Fig. 9).

Discussion

DOC and FDOM released by *P. tricornutum*

The DOC release pattern, observed during the growth of *P. tricornutum*, agrees with previous studies on the prymnesiophyte *Phaeocystis* sp. and the diatom *Skeletonema costatum*, for which a constant DOC release, independent on the growth phase, was observed (Biddanda and Benner 1997). In contrast, an increased DOC release during the declining growth phase of laboratory cultures was observed for *Synechococcus bacillaris* and *Emiliania huxleyi* (Biddanda and Benner 1997) and at the end of an experimental diatom bloom (Norrman et al. 1995; Obernosterer and Herndl 1995). Other studies reported high DOC release during the transition between exponential and stationary growth phase (Granum et al. 2002; Wetz and Wheeler 2007). The reason behind different DOC release patterns by different phytoplankton species is not clear. It has been reported that diatoms release different metabolites during growth phases (Barofsky et al. 2009; Vidoudez and Pohnert 2012). During bloom simulation experiments, a lower net production of DOM rich in N was reported in nutrient replete conditions compared to nutrient limited conditions (Wetz and Wheeler 2007). It has also been observed that the chemical composition of marine DOM depends on phytoplankton phylogeny and adaptations to a particular environment (Becker et al. 2014). Some phytoplankton species are mixotrophs and therefore they are able to take up part of the released photosynthates (Thornton 2014), masking the exudate release. Given these observations it is possible to hypothesize that the amount of DOC released during the different growth phases is dependent on the species used

for the experiments, its sensibility to nutrient conditions and capability of mixotrophy. However, we cannot exclude that in our experiment the lack of vitamins and trace metals in the culture media affected the amount and quality of DOM release by phytoplankton. The choice to use a medium free of vitamins and trace metals was done to minimize the occurrence of DOM in the medium, as reported by Grossart and Simon (2007), in order to better investigate the quality of DOM exclusively released by *P. tricornutum* without external contamination.

In contrast to DOC, the release of FDOM components was different in exponential and stationary growth phases. $C2_{Trp\text{-}like}$ fluorescence increased rapidly in the early exponential phase (i.e., after 2 d of incubation) and slowed after the transition into stationary phase (Fig. 2c). This observation suggests that the release of $C2_{Trp\text{-}like}$ can be a function of nutrient availability, with high release under nutrient-replete conditions (exponential growth phase) and low release under nutrient limitation (stationary phase). The observation that fluorescent protein-like material is released as a function of cell abundance agrees with past studies on the centric diatom *Thalassiosira pseudonana* (Longnecker et al. 2015) and with the observation that extracellular release of dissolved free amino acids by phytoplankton is species-dependent (Sarmento et al. 2013) and changes with growth phase and environmental conditions within a single species (Admiraal et al. 1986).

The release of flavin-like ($C1_{Flv\text{-}like}$) and humic-like ($C3_{H1\text{-}like}$ and $C4_{H2\text{-}like}$) substances started later compared to protein-like fluorophores ($C2_{Trp\text{-}like}$ and $C5_{Tyr\text{-}like}$; Fig. 2d, e and 3c). $C1_{Flv\text{-}like}$, $C3_{H1\text{-}like}$, and $C4_{H2\text{-}like}$ showed a good logarithmic relationship with the cell density ($R^2 > 0.95$, $p < 0.001$; Table 2), suggesting a greater release of these fluorophores during the stationary than the exponential growth phase.

It is noteworthy that the intensity of the fluorescence components shows a strong and significant linear correlation with DOC ($R^2 > 0.90$, $p < 0.05$; $C2_{Trp\text{-}like}$ $R^2 = 0.84$, $p < 0.05$; Table 2), indicating a coupling between DOC and FDOM production in our experimental conditions. This observation indicates a similar DOM composition at all the growth stages supporting the coupling between the release of DOC and FDOM during phytoplankton growth. The uncoupling, observed in the marine environment, is therefore mainly due to biotic (i.e., heterotrophic degradation) or abiotic (i.e., photobleaching) removal processes occurring in the water column after their release.

Biological lability of DOM released by *P. tricornutum*

DOC removal rates

In our study, the natural marine microbial community removed ~ 30% of the phytoplankton DOC in 24 d. This percentage is similar to that found by Zheng et al. (2019) (38%) and by Amon et al. (2001) (30%) but lower than that estimated by Romera-Castillo et al. (2011) (47–59%). Given that the quality of DOM released is dependent on phytoplankton phylogeny (Becker et al. 2014) and that different heterotrophic taxa have specialized metabolic and physiological adaptations to use specific compounds in DOM pool (Elovaara et al. 2021; Kieft et al. 2021), it is expected that the choice of the phytoplankton model organisms, as well as the microbial community inoculated into the exudates, affect the amount of DOC removed. The experimental conditions may also influence the exudate uptake. Romera-Castillo et al. (2011) used for the phytoplankton culture a medium with a high DOC content (192–233 μM), the initial DOC concentration in their incubation was much higher with respect to our study (59 μM) and to that of Zheng et al. (2019), suggesting that the

Table 2. Values of r^2 and p for the linear and logarithmic correlations among DOC, cell density, $C1_{Flv\text{-}like}$, $C2_{Trp\text{-}like}$, $C3_{H1\text{-}like}$, $C4_{H2\text{-}like}$, and $C5_{Tyr\text{-}like}$ during the phytoplankton growth.

	DOC (μM)	Cell density	$C1_{Flv\text{-}like}$	$C2_{Trp\text{-}like}$	$C3_{H1\text{-}like}$	$C4_{H2\text{-}like}$	$C5_{Tyr\text{-}like}$
DOC (μM)							
Cell density	0.80						
	$p = 0.04$						
$C1_{Flv\text{-}like}$	0.92	0.99*					
	$p = 0.009$	$p < 0.0001$					
$C2_{Trp\text{-}like}$	0.84	0.98	0.92				
	$p = 0.028$	$p < 0.001$	$p = 0.009$				
$C3_{H1\text{-}like}$	0.94	0.98*	0.99	0.91			
	$p = 0.005$	$p = 0.0002$	$p < 0.001$	$p = 0.011$			
$C4_{H2\text{-}like}$	0.95	0.95*	0.99	0.88	0.99		
	$p = 0.004$	$p = 0.0009$	$p < 0.001$	$p = 0.017$	$p < 0.001$		
$C5_{Tyr\text{-}like}$	0.97	0.68	0.90	0.75	0.92	0.95	
	$p = 0.002$	$p = 0.083$	$p = 0.014$	$p = 0.055$	$p = 0.010$	$p = 0.005$	

*Logarithmic correlation.

initial DOC concentration can affect DOC removal rates. In our experiment, we avoided this problem using a medium free of vitamins and trace metals with a very low DOC concentration.

In our experiment, immediately after inoculation, DOC concentration decreased exponentially in correspondence with an increase in HPA (Figs. 5, 6a). After the initial sharp decrease, DOC kept decreasing slowly and the HPA kept increasing until the last 3 d of the experiment when both DOC and HPA stabilized (Fig. 5). This trend is related to the quality of DOC; at the beginning of the experiment (between days 0 and 3) the high concentration of labile DOC supported the quick bacterial growth with high HPGE (33%), whereas between days 3 and 24, less labile compounds predominated slowing down the removal rates and the HPGE (12%). The lower HPGE during the second phase indicates a shift in the heterotrophic prokaryote community towards a maintenance metabolism, using more DOC for respiration than for biomass synthesis, when compared to the beginning of the incubation. This observation is in agreement with the literature, where high values of HPGE are often observed in eutrophic environments, whereas low values are associated with increased oligotrophy (Del Giorgio 2000; Carlson et al. 2002). Differences in HPGE have also been correlated with the quality of the substrate (Eiler et al. 2003) and, in our case, they are likely related to the change in DOM composition.

Lability of protein-like substances

Protein-like substances are usually considered part of the labile fraction of DOM (Lønborg et al. 2010; Casas-Ruiz et al. 2020), they are therefore not expected to persist in the ocean on a temporal scale of months-years. However, the widely used PARAFAC analysis applied to seawater samples show the presence of protein-like fluorescence everywhere in the oceans (Jørgensen et al. 2011; Catalá et al. 2015), indicating that, even if we cannot quantitatively estimate their concentration, a fraction of proteins persists in the oceans. Keil and Kirchman (1999) indeed observed that dissolved combined amino acids survives in surface waters long enough to be advected or overturned into the deep water where a fraction persists on the long temporal scale.

Our results support a high lability for the $C2_{Trp\text{-}like}$ and a coupling between its removal and the decrease in DOC ($r^2 = 0.95$, $p < 0.001$; Table 3). These results agree with past incubation experiments (Zheng et al. 2019) as well as with observations in the field (Jørgensen et al. 2011; Galletti et al. 2019), where protein-like fluorescence exhibits the same pattern as DOC concentration, with high values in the surface layer (0–200 m) and a general decrease with depth (200–2000 m), to reach low and constant values below ~ 2000 m. In contrast, $C5_{Tyr\text{-}like}$ does not correlate with DOC ($r^2 = 0.43$, $p = 0.078$; Table 3) and exhibits a marked increase during the first 3 d of incubation.

Major changes in protein hydrophobicity and molecular weight were also observed during the incubation (Figs. 7c, 8c, 9). We therefore posit that the decrease in $C2_{Trp\text{-}like}$ fluorescence and the increase in $C5_{Tyr\text{-}like}$ during the early incubation (Fig. 7c, 8c) are related to the transformation of high-molecular-weight proteins into small peptides. The initial increase in $C5_{Tyr\text{-}like}$ agrees with this hypothesis since in high-molecular-weight proteins, the fluorescence of tyrosine is masked by tryptophan but can increase as a result of the extracellular enzyme cleavage of proteins gradually exposing tyrosine (Yamashita and Tanoue 2004). This hypothesis is supported by the trend of the two protein-like components ($C2_{trp\text{-}like}$ and $C5_{Tyr\text{-}like}$) in the low- and high-molecular-weight fractions (Figs. 7c, 8c). It is noteworthy that in the HMWDOM $C5_{Tyr\text{-}like}$ decreased after the initial increase (Fig. 8c), indicating the

Table 3. Values of r^2 and p for the linear correlations among DOC, HPA, $C1_{Flv\text{-}like}$, $C2_{Trp\text{-}like}$, $C3_{H1\text{-}like}$, $C4_{H2\text{-}like}$, and $C5_{Tyr\text{-}like}$ during the incubation experiment.

	DOC (μM)	HPA	$C1_{Flv\text{-}like}$	$C2_{Trp\text{-}like}$	$C3_{H1\text{-}like}$	$C4_{H2\text{-}like}$	$C5_{Tyr\text{-}like}$
DOC (μM)							
HPA	0.95						
	$p < 0.001$						
$C1_{Flv\text{-}like}$	0.90	0.91					
	$p < 0.001$	$p < 0.001$					
$C2_{Trp\text{-}like}$	0.95	0.96	0.94				
	$p < 0.001$	$p < 0.001$	$p < 0.001$				
$C3_{H1\text{-}like}$	0.53	0.54	0.31	0.46			
	$p = 0.040$	$p = 0.024$	$p = 0.113$	$p = 0.043$			
$C4_{H2\text{-}like}$	0.16	0.04	0.20	0.14	0.01		
	$p = 0.326$	$p = 0.568$	$p = 0.222$	$p = 0.313$	$p = 0.775$		
$C5_{Tyr\text{-}like}$	0.42	0.30	0.46	0.41	0.004	0.38	
	$p = 0.078$	$p = 0.126$	$p = 0.043$	$p = 0.062$	$p = 0.868$	$p = 0.076$	

removal of these fluorophores. It is important to notice that the initial increase in low-molecular-weight peptides does not imply that their removal did not occur at all during the first days, but that the small peptides produced by the breakdown of high-molecular-weight proteins exceed those eventually removed by the bacterial community.

The HPLC analysis of high-molecular-weight proteins shows a marked decrease in the hydrophobic (nonpolar) proteins and a shift of the peaks at 1.9 and 2.9 min, attributed to hydrophilic (polar) proteins, to a unique hydrophilic peak at 2.5 min (Fig. 9). It is noteworthy that, since no difference was observed in the control, abiotic processes can be excluded as drivers of the observed change in polarity. The HPLC results can be interpreted in two ways: (1) heterotrophic prokaryotes remove preferentially the hydrophobic high-molecular-weight proteins, suggesting a link between polarity and lability with higher lability of hydrophobic than hydrophilic proteins. (2) hydrophobic high-molecular-weight proteins are cut exposing the hydrophilic part with a consequent shift in the peaks.

Within the high-molecular-weight fraction, the shift in the hydrophobicity of the proteins agrees with the fluorescence data and indicate a partitioning in the uptake of protein-like exudates with different molecular weight and polarity. Our data show that despite the high biological lability of most of the released proteins, polarity and molecular weight affects their dynamics of uptake. Heterotrophic prokaryote degradation of the phytoplankton-produced protein-like material is a highly selective process that preferentially consume high-molecular-weight hydrophobic molecules and transform them into low-molecular-weight hydrophilic peptides.

The possible implications of our observations need more in-depth studies, focusing on the metabolic and physiologic consequences of the use of hydrophobic high-molecular-weight proteins with respect to hydrophilic low-molecular-weight substrates. Past studies have already provided evidences that different phytoplankton exudates provide lineage-specific rates of carbon assimilation (Kieft et al. 2021). If the characteristics of the substrate are so crucial in the partitioning of the microbial communities, changes in the percentage of the high-molecular-weight proteins released by phytoplankton could shape the heterotrophic prokaryote communities with consequences for the microbial loop and the global carbon cycle.

Lability of humic-like substances

Humic-like substances constitute a heterogeneous mixture of acidic and highly aromatic compounds with different origins (Tranvik 1998), recent studies indicated that about 50% of the total DOC in the ocean is comprised of humic-like substances resistant to bacterial degradation (Zigah et al. 2017). Humic-like substances exhibit a wide range of molecular weight from less than 500 Da to greater than 10,000 Da (Perminova et al. 2003). Past studies highlighted their relatively low molecular weight, even if dynamic hydrophobic interactions can form supramolecular structures with an apparent high molecular weight (Batchelli et al. 2009; Muller 2018). Our results support the low molecular weight of humic-like substances. Even if past studies pointed out the recalcitrance of humic-like substances to bacterial degradation (Moran and Hodson 1990), the biological lability of these substances is still under debate. Estimates of terrestrial DOC turnover times based on lignin phenol content (Opsahl and Benner 1998) suggest a quick degradation of humic material of terrestrial origin, but there is no way to disentangle the biotic (mineralization) and abiotic (photobleaching) removal processes in the open oceans. Regarding the humic-like substances released by phytoplankton, the literature is scarce and suggests a substantial stability over time (Romera-Castillo et al. 2011; Zheng et al. 2019); however, Romera-Castillo et al. (2011) did observe the removal of humic-like substances (peak-M) released by the diatom *Sk. costatum*. Our results supports that some humic-like substances ($C3_{H1\text{-}like}$) are stable on the short temporal scale. The slight increase in $C3_{H1\text{-}like}$ in the first 4 d of incubation, agrees with previous studies where an increase in humic-like fluorescence was observed during incubation of phytoplankton DOM with a marine heterotrophic prokaryote community (Romera-Castillo et al. 2010; Fukuzaki et al. 2014). An increase in humic-like fluorescence was also observed in aged waters in the oceans and attributed to heterotrophic microbial activity (Chen and Bada 1992; Yamashita and Tanoue 2008; Yamashita et al. 2010).

The trend of $C4_{H2\text{-}like}$ fluorescence was unexpected. It increased within the first 7 d of incubation and then decreased to return to its initial values (Fig. 8a). A similar trend was also observed by other authors in incubation using *Synechococcus*-derived DOM (Zheng et al. 2019). These results are also in agreement with a study showing that the humic-like substances are used only after the consumption of more labile substrates (Shimotori et al. 2009); thus, after being released during the first days of incubation, $C4_{H2\text{-}like}$ was likely utilized by the heterotrophic prokaryotes, once the labile substances were removed.

Lability of HMWDOM

Our data indicate that 75% of DOC released by *P. tricornutum* was low molecular weight, whereas only 25% was high molecular weight. These percentages reflect those found in the oceans, where the vast majority (~ 77%) of DOC resides in the size class of dissolved molecules lower than 1000 Da (Benner and Amon 2015). If compared with other culture experiments, the percentage of HMWDOM well agrees with those reported by Biddanda and Benner (1997), who observed that HMWDOM accounted for 35% (*Sy. bacillaris*, 36%; *Phaeocystis* sp., 31%; *E. huxleyi*, 36%; *Sk. costatum*, 38%) of the released DOC.

At the end of our incubation experiment, 20% of the HMWDOM and 40% of the LMWDOM were removed, making

LMWDOM still 70% of the total DOM. It is important to notice that the percentages of LMWDOM removed may have been underestimated if some low-molecular-weight compounds were produced by the degradation of high-molecular-weight compounds. However, we cannot completely exclude some aggregation processes producing HMWDOM from low-molecular-weight substrates. The half-life time observed for the labile fraction of HMWDOM was the shortest (0.5 d; Table 1), suggesting high biological lability of some molecules bigger than 3000 Da. The high reactivity of a fraction of HMWDOM is related to the ability of a considerable fraction of surface marine heterotrophic prokaryotes to specifically and rapidly bind high-molecular-weight substrates (Arnosti et al. 2018). However, after the quick initial decrease, 75% of HMWDOM (43 ± 4 μM) persisted over the incubation, indicating that a major part of this fraction was not labile over the 24 d of incubation. HMWDOM is known to be rich in carbohydrates (Benner and Amon 2015; Arnosti et al. 2018), up to 70% of the HMWDOM recovered by ultrafiltration consists of acyl polysaccharides that are resistant to microbial degradation (Repeta 2015). The observation that the majority of HMWDOM, released by *P. tricornutum*, persisted in our incubations suggests that most of it could be comprised of a carbohydrate-rich mixture of compounds that persist for months to years in the oceans. In order to support this hypothesis, total dissolved polysaccharides were determined in the total DOM with the spectrophotometric method using the reagent 2,4,6-tripyridil-s-triazine (*see* the Supporting Information Fig. S3; Myklestad et al. 1997). A substantial stability of their concentration was observed during the 24 d of incubation (Supporting Information Fig. S4). We speculate that the rapid decrease in HMWDOM concentration is mostly related to the uptake and degradation of proteins by the microbial community. Indeed proteins constitutes a significant portion of the released DOM (Myklestad 2000; Granum et al. 2002; Thornton 2014) and, as seen from the FDOM trend (Fig. 7c), the protein-like fluorescence in the high-molecular-weight fraction sharply decreases during the first days of incubation. Further studies on the degradation of freshly produced proteins are needed, but our results suggest that proteins are quickly removed fueling the bacterial community during the early exponential growth phase.

Lability of LMWDOM

The labile fraction of LMWDOM exhibited a half-life time (10.7 d; Table 1) longer than the labile fraction of HMWDOM with slow and continuous removal over the entire incubation (Fig. 6; Table 1). In the literature, the biological lability of this fraction is controversial, most of the oceanic DOM is known to be comprised of low-molecular-weight molecules resistant to microbial degradation, therefore persisting for years to millennia in the oceans (Hansell 2013; Benner and Amon 2015; Walker et al. 2016). In our study, 40% of LMWDOM was removed after 24 d of incubation, indicating high reactivity of LMWDOM released by *P. tricornutum*. At the end of the incubation, the percentages of HMWDOM and LMWDOM were similar to those observed at the beginning, 70% and 30%, respectively. These results point out that, a fraction of HMWDOM is highly labile and rapidly removed in few days (i.e., high removal rates and small half-life time). However, over the timescale of our experiment, the proportion of high- and low-molecular-weight DOM did not change, suggesting no real link between lability and molecular weight on the time scale of our incubations.

Production of flavin-like fluorophores

The first PARAFAC component ($C1_{Flv\text{-}like}$) showed spectroscopic characteristics similar to that of the riboflavin (vitamin B2) and lumichrome (Wünsch et al. 2015; Yang et al. 2016). The exudation of this fluorophore by *P. tricornutum* (Seritti et al. 1994), was unexpected since both eukaryotic phytoplankton and bacterioplankton are auxotrophic for at least one B vitamin, mainly because they lack the complete biosynthetic pathways required to produce them (Giovannoni et al. 2005). Studies on the vitamin B2 and its derivatives in the open ocean are scarce, but the few papers published highlight the very low concentration of these compounds in the water column (Sañudo-Wilhelmy et al. 2012; Monteverde et al. 2018), indicating that in large areas of the ocean, the efficiency of the biological pump may be controlled by vitamins concentration and not only by nutrient limitation (Sañudo-Wilhelmy et al. 2012). The good correlation between the production of $C1_{Flv\text{-}like}$, $C3_{H1\text{-}like}$ and $C4_{H2\text{-}like}$ (Table 2) suggests that during the phytoplankton growth, the release of flavins follows that of the humic-like substances, in agreement with some studies suggesting that flavins may represent a common component of the humic-like fraction in aqueous systems (Borch et al. 2010). In the open ocean, the $C1_{Flv\text{-}like}$ may be released and immediately degraded by biotic/abiotic processes, hindering to observed its recalcitrance. In the HMWDOM, the $C1_{Flv\text{-}like}$ signal was very low with respect to the total DOM and the LMWDOM, suggesting that most of this fluorophore was in the LMWDOM, in agreement with the low molecular weight of riboflavin.

Conclusions

Our results indicate that *P. tricornutum* constantly releases both DOC and FDOM (protein-like, humic-like and flavin-like compounds) during its growth and that freshly produced phytoplankton DOM exhibits a dynamic pattern of degradation, highly dependent on its quality. Twenty-five percent of phytoplankton DOM is high molecular weight and 20% of it is quickly removed when exposed to marine bacteria. Low-molecular-weight DOM is 75% of phytoplankton DOM and is removed slowly, still representing 70% of the total DOM pool after 24 d of incubation. During the incubation, the growth efficiency of the bacterial community was high (33%) during the first 3 d and decreased to 12% once the most labile

compounds were removed, suggesting that the quality of DOM affects microbial metabolism and that once the labile DOM is removed there is a shift in the heterotrophic prokaryote community toward a maintenance metabolism.

Fluorescence data indicate high lability of protein-like fluorescent DOM and confirms that humic-like substances are resistant to bacterial degradation on the temporal scale of weeks.

Flavin-like fluorophores, compounds of the B vitamin group, present at extremely low concentration in the ocean, are released as the most representative FDOM fluorophores by *P. tricornutum*, suggesting that in nature they are released only by specific phytoplankton strains or that they are maintained at low concentration by biotic/abiotic processes.

The separation of the phytoplankton DOM into low- and high-molecular-weight fractions combined with HPLC analysis provided evidence for the degradation of proteins > 3000 Da into small peptides during the first days of incubation, concurrent with the transformation of hydrophobic proteins to more hydrophilic ones. Although it may seem speculative, these results indicate that once released by phytoplankton, high-molecular-weight proteins are preferentially mineralized by the microbial community and undergo a variety of transformations that alter their hydrophobicity. Proteins and amino acids represent an important source of labile organic substrates for the bacterial communities in the ocean, recent global models predict a nonlinearity behavior of DOM in response to environmental changes with less organic matter accumulating and a shift towards a more dynamic and labile DOM pool in a warmer ocean (Zakem et al. 2021). In this perspective, studies aimed to better identify the main drivers of DOM lability as well as the link between DOM quality and bacterial growth efficiency are crucial.

Data availability statement

All the data are reported in the Supporting Information (Tables S3–S5).

References

Admiraal, W., H. Peletier, and R. W. P. M. Laane. 1986. Nitrogen metabolism of marine planktonic diatoms; excretion, assimilation and cellular pools of free amino acids in seven species with different cell size. J. Exp. Mar. Biol. Ecol. **98**: 241–263. doi:10.1016/0022-0981(86)90216-9

Amon, R. M. W., and R. Benner. 1994. Rapid cycling of high-molecular-weight dissolved organic matter in the ocean. Nature **369**: 549–552. doi:10.1038/369549a0

Amon, R. M. W., H.-P. Fitznar, and R. Benner. 2001. Linkages among the bioreactivity, chemical composition, and diagenetic state of marine dissolved organic matter. Limnol. Oceanogr. **46**: 287–297. doi:10.4319/lo.2001.46.2.0287

Arnosti, C., G. Reintjes, and R. Amann. 2018. A mechanistic microbial underpinning for the size-reactivity continuum of dissolved organic carbon degradation. Mar. Chem. **206**: 93–99. doi:10.1016/j.marchem.2018.09.008

Balestra, C., L. Alonso-sáez, J. M. Gasol, and R. Casotti. 2011. Group-specific effects on coastal bacterioplankton of polyunsaturated aldehydes produced by diatoms. Aquat. Microb. Ecol. **63**: 123–131. doi:10.3354/ame01486

Barofsky, A., C. Vidoudez, and G. Pohnert. 2009. Metabolic profiling reveals growth stage variability in diatom exudates. Limnol. Oceanogr. Methods **7**: 382–390. doi:10.4319/lom.2009.7.382

Batchelli, S., F. L. L. Muller, M. Baalousha, and J. R. Lead. 2009. Size fractionation and optical properties of colloids in an organic-rich estuary (Thurso, UK). Mar. Chem. **113**: 227–237. doi:10.1016/j.marchem.2009.02.006

Becker, J. W., P. M. Berube, C. L. Follett, J. B. Waterbury, S. W. Chisholm, E. F. DeLong, and D. J. Repeta. 2014. Closely related phytoplankton species produce similar suites of dissolved organic matter. Front. Microbiol. **5**: 1–14 doi:10.3389/fmicb.2014.00111

Benner, R., and R. M. W. Amon. 2015. The size-reactivity continuum of major bioelements in the ocean. Ann. Rev. Mar. Sci. **7**: 185–205. doi:10.1146/annurev-marine-010213-135126

Bennette, N. B., J. F. Eng, and G. C. Dismukes. 2011. An LC–MS-based chemical and analytical method for targeted metabolite quantification in the model cyanobacterium *Synechococcus* sp. PCC 7002. Anal. Chem. **83**: 3808–3816. doi:10.1021/ac200108a

Biddanda, B., and R. Benner. 1997. Carbon, nitrogen, and carbohydrate fluxes during the production of particulate and dissolved organic matter by marine phytoplankton. Limnol. Oceanogr. **42**: 506–518. doi:10.4319/lo.1997.42.3.0506

Borch, T., R. Kretzschmar, A. Kappler, P. Van Cappellen, M. Ginder-Vogel, A. Voegelin, and K. Campbell. 2010. Biogeochemical redox processes and their impact on contaminant dynamics. Environ. Sci. Technol. **44**: 15–23. doi:10.1021/es9026248

Bromke, M. A., P. Giavalisco, L. Willmitzer, and H. Hesse. 2013. Metabolic analysis of adaptation to short-term changes in culture conditions of the marine diatom *Thalassiosira pseudonana*. PLoS One **8**: e67340. doi:10.1371/journal.pone.0067340

Butler, T., R. V. Kapoore, and S. Vaidyanathan. 2020. *Phaeodactylum tricornutum*: A diatom cell factory. Trends Biotechnol. **38**: 606–622. doi:10.1016/j.tibtech.2019.12.023

Carlson, C. A., S. J. Giovannoni, D. A. Hansell, S. J. Goldberg, R. Parsons, M. P. Otero, and K. Vergin. 2002. Effect of nutrient amendments on bacterioplankton production, community structure, and DOC utilization in the northwestern Sargasso Sea. Aquat. Microb. Ecol. **30**: 19–36.

Casas-Ruiz, J. P., and others. 2020. Delineating the continuum of dissolved organic matter in temperate river networks. Global Biogeochem. Cycl. **34**: 1–15. doi:10.1029/2019GB006495

Catalá, T. S., and others. 2015. Water mass age and aging driving chromophoric dissolved organic matter in the dark global ocean. Global Biogeochem. Cycl. **29**: 917–934. doi:10.1002/2014GB005048

Chen, R. F., and J. L. Bada. 1992. The fluorescence of dissolved organic matter in seawater. Mar. Chem. **37**: 191–221. doi:10.1016/0304-4203(92)90078-O

Coble, P. G. 1996. Characterization of marine and terrestrial DOM in seawater using excitation-emission matrix spectroscopy. Mar. Chem. **51**: 325–346. doi:10.1016/0304-4203(95)00062-3

Coble, P. G., C. E. Del Castillo, and B. Avril. 1998. Distribution and optical properties of CDOM in the Arabian Sea during the 1995 southwest monsoon. Deep Sea Res. Part II Top. Stud. Oceanogr. **45**: 2195–2223. doi:10.1016/S0967-0645(98)00068-X

Del Giorgio, P. A. 2000. Bacterial energetics and growth efficiency, p. 289–325. *In* Microbial ecology of the oceans. Wiley-Liss.

Eiler, A., S. Langenheder, S. Bertilsson, and L. J. Tranvik. 2003. Heterotrophic bacterial growth efficiency and community structure at different natural organic carbon concentrations. Appl. Environ. Microbiol. **69**: 3701–3709. doi:10.1128/AEM.69.7.3701-3709.2003

Elovaara, S., E. Eronen-Rasimus, E. Asmala, T. Tamelander, and H. Kaartokallio. 2021. Contrasting patterns of carbon cycling and dissolved organic matter processing in two phytoplankton–bacteria communities. Biogeosciences **18**: 6589–6616. doi:10.5194/bg-18-6589-2021

Fukuda, R., H. Ogawa, T. Nagata, and I. Koike. 1998. Direct determination of carbon and nitrogen contents of natural bacterial assemblages in marine environments. Appl. Environ. Microbiol. **64**: 3352–3358. doi:10.1128/AEM.64.9.3352-3358.1998

Fukuzaki, K., I. Imai, K. Fukushima, K.-I. Ishii, S. Sawayama, and T. Yoshioka. 2014. Fluorescent characteristics of dissolved organic matter produced by bloom-forming coastal phytoplankton. J. Plankton Res. **36**: 685–694. doi:10.1093/plankt/fbu015

Galletti, Y., M. Gonnelli, S. Retelletti Brogi, S. Vestri, and C. Santinelli. 2019. DOM dynamics in open waters of the Mediterranean Sea: New insights from optical properties. Deep Sea Res. Part I Oceanogr. Res. Pap. **144**: 95–114. doi:10.1016/j.dsr.2019.01.007

Giovannoni, S. J., and others. 2005. Genome streamlining in a cosmopolitan oceanic bacterium. Science **309**: 1242–1245. doi:10.1126/science.1114057

Granum, E., S. Kirkvold, and S. Myklestad. 2002. Cellular and extracellular production of carbohydrates and amino acids by the marine diatom *Skeletonema costatum*: Diel variations and effects of N depletion. Mar. Ecol. Ser. **242**: 83–94. doi:10.3354/meps242083

Grossart, H., and M. Simon. 2007. Interactions of planktonic algae and bacteria: Effects on algal growth and organic matter dynamics. Aquat. Microb. Ecol. **47**: 163–176. doi:10.3354/ame047163

Grossart, H.-P., F. Levold, M. Allgaier, M. Simon, and T. Brinkhoff. 2005. Marine diatom species harbour distinct bacterial communities. Environ. Microbiol. **7**: 860–873. doi:10.1111/j.1462-2920.2005.00759.x

Hansell, D. A. 2005. Dissolved organic carbon reference material program. Eos Trans. Am. Geophys. Union **86**: 318. doi:10.1029/2005EO350003

Hansell, D. A. 2013. Recalcitrant dissolved organic carbon fractions. Ann. Rev. Mar. Sci. **5**: 421–445. doi:10.1146/annurev-marine-120710-100757

Jørgensen, L., C. A. Stedmon, T. Kragh, S. Markager, M. Middelboe, and M. Søndergaard. 2011. Global trends in the fluorescence characteristics and distribution of marine dissolved organic matter. Mar. Chem. **126**: 139–148. doi:10.1016/j.marchem.2011.05.002

Keil, R., and D. Kirchman. 1999. Utilization of dissolved protein and amino acids in the northern Sargasso Sea. Aquat. Microb. Ecol. **18**: 293–300. doi:10.3354/ame018293

Kieft, B., Z. Li, S. Bryson, R. L. Hettich, C. Pan, X. Mayali, and R. S. Mueller. 2021. Phytoplankton exudates and lysates support distinct microbial consortia with specialized metabolic and ecophysiological traits. Proc. Natl. Acad. Sci. U.S.A. **118**: e2101178118. doi:10.1073/pnas.2101178118

Kinsey, J. D., G. Corradino, K. Ziervogel, A. Schnetzer, and C. L. Osburn. 2018. Formation of chromophoric dissolved organic matter by bacterial degradation of phytoplankton-derived aggregates. Front. Mar. Sci. **4**: 430. doi:10.3389/fmars.2017.00430

Lancelot, C. 1984. Extracellular release of small and large molecules by phytoplankton in the Southern Bight of the North Sea. Estuar. Coast. Shelf Sci. **18**: 65–77. doi:10.1016/0272-7714(84)90007-6

Lawaetz, A. J., and C. A. Stedmon. 2009. Fluorescence intensity calibration using the Raman scatter peak of water. Appl. Spectrosc. **63**: 936–940. doi:10.1366/000370209788964548

Lønborg, C., X. A. Álvarez-Salgado, K. Davidson, S. Martínez-García, and E. Teira. 2010. Assessing the microbial bioavailability and degradation rate constants of dissolved organic matter by fluorescence spectroscopy in the coastal upwelling system of the Ría de Vigo. Mar. Chem. **119**: 121–129. doi:10.1016/j.marchem.2010.02.001

Longnecker, K., M. C. Kido Soule, and E. B. Kujawinski. 2015. Dissolved organic matter produced by *Thalassiosira pseudonana*. Mar. Chem. **168**: 114–123. doi:10.1016/j.marchem.2014.11.003

Mentges, A., C. Feenders, C. Deutsch, B. Blasius, and T. Dittmar. 2019. Long-term stability of marine dissolved organic carbon emerges from a neutral network of compounds and microbes. Sci. Rep. **9**: 17780. doi:10.1038/s41598-019-54290-z

Monteverde, D. R., J. B. Sylvan, C. Suffridge, J. J. Baronas, E. Fichot, J. Fuhrman, W. Berelson, and S. A. Sañudo-Wilhelmy.

2018. Distribution of extracellular flavins in a coastal marine basin and their relationship to redox gradients and microbial community members. Environ. Sci. Technol. **52**: 12265–12274. doi:10.1021/acs.est.8b02822

Moran, M. A., and R. E. Hodson. 1990. Bacterial production on humic and nonhumic components of dissolved organic carbon. Limnol. Oceanogr. **35**: 1744–1756. doi:10.4319/lo.1990.35.8.1744

Muller, F. L. L. 2018. Exploring the potential role of terrestrially derived humic substances in the marine biogeochemistry of iron. Front. Earth Sci. **6**: 1–20. doi:10.3389/feart.2018.00159

Murphy, K. R., C. A. Stedmon, D. Graeber, and R. Bro. 2013. Fluorescence spectroscopy and multi-way techniques. PARAFAC. Anal. Methods **5**: 6557–6566. doi:10.1039/c3ay41160e

Murphy, K. R., C. A. Stedmon, P. Wenig, and R. Bro. 2014. OpenFluor– An online spectral library of auto-fluorescence by organic compounds in the environment. Anal. Methods **6**: 658–661. doi:10.1039/C3AY41935E

Myklestad, S. M. 2000. Dissolved organic carbon from phytoplankton, p. 111–148. *In* P. J. Wangersky [ed.], Marine chemistry. Springer.

Myklestad, S. M., E. Skånøy, and S. Hestmann. 1997. A sensitive and rapid method for analysis of dissolved mono- and polysaccharides in seawater. Mar. Chem. **56**: 279–286. doi:10.1016/S0304-4203(96)00074-6

Norrman, B., U. L. Zwelfel, C. S. Hopkinson, and F. Brian. 1995. Production and utilization of dissolved organic carbon during an experimental diatom bloom. Limnol. Oceanogr. **40**: 898–907. doi:10.4319/lo.1995.40.5.0898

Obernosterer, I., and G. Herndl. 1995. Phytoplankton extracellular release and bacterial growth: Dependence on the inorganic N:P ratio. Mar. Ecol. Prog. Ser. **116**: 247–257. doi:10.3354/meps116247

Opsahl, S., and R. Benner. 1998. Photochemical reactivity of dissolved lignin in river and ocean waters. Limnol. Oceanogr. **43**: 1297–1304. doi:10.4319/lo.1998.43.6.1297

Paul, C., A. Barofsky, C. Vidoudez, and G. Pohnert. 2009. Diatom exudates influence metabolism and cell growth of cocultured diatom species. Mar. Ecol. Prog. Ser. **389**: 61–70. doi:10.3354/meps08162

Perminova, I. V., F. H. Frimmel, A. V. Kudryavtsev, N. A. Kulikova, G. Abbt-Braun, S. Hesse, and V. S. Petrosyan. 2003. Molecular weight characteristics of humic substances from different environments as determined by size exclusion chromatography and their statistical evaluation. Environ. Sci. Technol. **37**: 2477–2485. doi:10.1021/es0258069

Repeta, D. J. 2015. Chemical characterization and cycling of dissolved organic matter, p. 21–63. *In* D. A. Hansell and C. A. Carlson [eds.], Biogeochemistry of marine dissolved organic matter. Academic Press.

Romera-Castillo, C., H. Sarmento, X. A. Álvarez-Salgado, J. M. Gasol, and C. Marrasé. 2010. Production of chromophoric dissolved organic matter by marine phytoplankton. Limnol. Oceanogr. **55**: 446–454. doi:10.4319/lo.2010.55.1.0446

Romera-Castillo, C., H. Sarmento, X. A. Álvarez-Salgado, J. M. Gasol, and C. Marrasé. 2011. Net production and consumption of fluorescent colored dissolved organic matter by natural bacterial assemblages growing on marine phytoplankton exudates. Appl. Environ. Microbiol. **77**: 7490–7498. doi:10.1128/AEM.00200-11

Sañudo-Wilhelmy, S. A., and others. 2012. Multiple B-vitamin depletion in large areas of the coastal ocean. Proc. Natl. Acad. Sci. U.S.A. **109**: 14041–14045. doi:10.1073/pnas.1208755109

Sarmento, H., C. Romera-Castillo, M. Lindh, J. Pinhassi, M. M. Sala, J. M. Gasol, C. Marrassé, and G. T. Taylor. 2013. Phytoplankton species-specific release of dissolved free amino acids and their selective consumption by bacteria. Limnol. Oceanogr. **58**: 1123–1135. doi:10.4319/lo.2013.58.3.1123

Seritti, A., E. Morelli, L. Nannicini, and R. Del Vecchio. 1994. Production of hydrophobic fluorescent organic matter by the marine diatom *Phaeodactylum tricornutum*. Chemosphere **28**: 117–129. doi:10.1016/0045-6535(94)90205-4

Shimotori, K., Y. Omori, and T. Hama. 2009. Bacterial production of marine humic-like fluorescent dissolved organic matter and its biogeochemical importance. Aquat. Microb. Ecol. **58**: 55–66.

Sipler, R. E., and D. A. Bronk. 2015. Dynamics of dissolved organic nitrogen, p. 127–232. *In* Biogeochemistry of marine dissolved organic matter. Elsevier.

Stedmon, C. A., and S. Markager. 2005. Tracing the production and degradation of autochthonous fractions of dissolved organic matter by fluorescence analysis. Limnol. Oceanogr. **50**: 1415–1426. doi:10.4319/lo.2005.50.5.1415

Thornton, D. C. O. 2014. Dissolved organic matter (DOM) release by phytoplankton in the contemporary and future ocean. Eur. J. Phycol. **49**: 20–46. doi:10.1080/09670262.2013.875596

Tranvik, L. J. 1998. Degradation of dissolved organic matter in humic waters by bacteria, p. 259–283. *In* Aquatic humic substances. Ecological studies, v. **133**. Springer.

Vidoudez, C., and G. Pohnert. 2012. Comparative metabolomics of the diatom *Skeletonema marinoi* in different growth phases. Metabolomics **8**: 654–669. doi:10.1007/s11306-011-0356-6

Walker, B. D., F. W. Primeau, S. R. Beaupré, T. P. Guilderson, E. R. M. Druffel, and M. D. McCarthy. 2016. Linked changes in marine dissolved organic carbon molecular size and radiocarbon age. Geophys. Res. Lett. **43**: 10385–10393. doi:10.1002/2016GL070359

Wetz, M. S., and P. A. Wheeler. 2007. Release of dissolved organic matter by coastal diatoms. Limnol. Oceanogr. **52**: 798–807. doi:10.4319/lo.2007.52.2.0798

Wünsch, U. J., K. R. Murphy, and C. A. Stedmon. 2015. Fluorescence quantum yields of natural organic matter and

organic compounds: Implications for the fluorescence-based interpretation of organic matter composition. Front. Mar. Sci. **2**: 98. doi:10.3389/fmars.2015.00098

Yamashita, Y., and E. Tanoue. 2004. Chemical characteristics of amino acid-containing dissolved organic matter in seawater. Org. Geochem. **35**: 679–692. doi:10.1016/j.orggeochem.2004.02.007

Yamashita, Y., and E. Tanoue. 2008. Production of bio-refractory fluorescent dissolved organic matter in the ocean interior. Nat. Geosci. **1**: 579–582.

Yamashita, Y., L. J. Scinto, N. Maie, and R. Jaffé. 2010. Dissolved organic matter characteristics across a subtropical wetland's landscape: application of optical properties in the assessment of environmental dynamics. Ecosystems **13**: 1006–1019. doi:10.1007/s10021-010-9370-1

Yang, H., X. Xiao, X. Zhao, L. Hu, C. Lv, and Z. Yin. 2016. Study on fluorescence spectra of thiamine, riboflavin and pyridoxine. MATEC Web Conf. **63**: 03013. doi:10.1117/12.2211248

Zakem, E. J., B. B. Cael, and N. M. Levine. 2021. A unified theory for organic matter accumulation. Proc. Natl. Acad. Sci. U.S.A. **118**: e2016896118. doi:10.1073/pnas.2016896118

Zheng, Q., Q. Chen, R. Cai, C. Chen, and N. Jiao. 2019. Molecular characteristics of microbially mediated transformations of Synechococcus-derived dissolved organic matter as revealed by incubation experiments. Sci. Total Environ. **21**: 2533–2543. doi:10.1111/1462-2920.14646

Zigah, P. K., A. P. McNichol, L. Xu, C. Johnson, C. Santinelli, D. M. Karl, and D. J. Repeta. 2017. Allochthonous sources and dynamic cycling of ocean dissolved organic carbon revealed by carbon isotopes. Geophys. Res. Lett. **44**: 2407–2415. doi:10.1002/2016GL071348

Acknowledgments

The authors are grateful to the two anonymous reviewers and the Associate Editor for the constructive remarks and suggestions who helped us to strongly improve the manuscript. This work was funded by the Gordon and Betty Moore Foundation (Grant GBMF3298) to C.S. and D.J.R., and Simons Foundation SCOPE program (Awards 621513, 329108) to D.J.R. The short-term mobility fellowship funded by CNR supported the visit of D.J.R. to the CNR giving the possibility to work on this paper. The authors are grateful to C. Neri, R. Cascone, R. Claps (IBF-CNR, Italy) for the assistance in the financial management. Open Access Funding provided by Consiglio Nazionale delle Ricerche within the CRUI-CARE Agreement.

Conflict of Interest

None declared.

Submitted 14 January 2022
Revised 16 September 2022
Accepted 05 February 2023

Associate editor: Hans-Peter Grossart